Geochemical Constraints on the Origin of Volcanic Rocks from the Andean Northern Volcanic Zone, Ecuador

J.A. Bryant (1)
G.M. Yogodzinski*(1)
M.L. Hall (2)
J.L. Lewicki (3)
D.G. Bailey (4)

(1) Department of Geological Sciences, University of South Carolina, 700 Sumter Street, Columbia, SC, 29208

(2) Instituto Geofisico, Escuela Politecnica Nacional (IG-EPN), Apartado 17-01-2759 Quito, Ecuador

(3) Earth Sciences Division, Lawrence Berkeley National Laboratory, 1 Cyclotron Road, Berkeley, CA 74720

(4) Department of Geology, Hamilton College, Clinton, NY

*corresponding author
Telephone: 001-803-777-9524
Fax: 001-803-777-6610
Email: gene@sc.edu

Keywords: andesite, Ecuador, trace elements, isotopes, adakite

ABSTRACT

Whole-rock geochemical data on basaltic to rhyolitic samples from 12 late Pleistocene-Holocene centers are used to constrain the role of continental crust in the genesis of melts formed beneath the anomalously wide arc in Ecuador. Primitive and relatively homogeneous isotopic compositions observed across the arc imply that Ecuador lavas were produced largely within the subduction zone and not by extensive melting of crustal rocks similar to those upon-which the volcanoes were built. Mixing calculations limit the quantity of assimilated crust to less than approximately 10%. Cross-arc geochemical variation (e.g., in $^{143}Nd/^{144}Nd$, Ba/Nb, La/Yb) indicates that assimilation of crustal rock is most active in the center-arc area, around the Inter-Andean Graben, at distances from 330-360 km from the trench. Characteristically 'adakitic' features (low Y, Yb, high La/Yb), which are observed in virtually all andesites and dacites in Ecuador as well as throughout the central and southern Andes, appear to be strongly influenced by crystal fractionation (e.g., as indicated by compatible element behavior for Y) and are most clearly developed in lavas that, based on isotopic compositions, have assimilated the most crust. A subset of andesites, which display an unusual combination of high Sr (>900 ppm) and non-radiogenic isotopes ($\varepsilon Nd > 4.1$, $\Delta 7/4Pb < 6.0$), appear to be regionally distinctive in Ecuador (i.e., not observed among modern lavas in the Andean central and southern volcanic zones or in Colombia). Only these lavas, which are well represented at Imbabura Volcano, appear to have geochemical features that may be consistent with a slab-melt interpretation associated with the subduction of relatively young, over-thickened oceanic crust of the subducting Carnegie Ridge.

INTRODUCTION

It is widely believed that subduction-related andesite forms predominantly through the evolution of basaltic melts and their interaction with arc crust (e.g., Gill, 1981; James & Murcia, 1984). In oceanic settings, where the arc crust is thin, the contribution of crustal material to the formation of lavas is often minimal, and andesites are viewed as secondary products of basalt evolution by crystal fractionation and magma mixing (Gill, 1981; Conrad & Kay, 1984; Woodhead, 1988; Singer & Myers, 1990). This model for andesite genesis in island arcs is central to our understanding of subduction magmatism and has played a significant role in the development of ideas on the formation and evolution of continental crust in subduction zones (e.g., Kay & Kay, 1991; Kelemen, 1995; Holbrook *et al.,* 1999).

An alternative view of arc magmatism and andesite genesis has recently grown out of the recognition that in some arcs, especially in places where subducting oceanic crust is young and/or warm, calc-alkaline andesite and dacite may form not only through the evolution of basaltic melts, but also through the melting of basaltic sources at high pressures in subducting oceanic crust (Kay, 1978; Saunders et al., 1987; Defant & Drummond, 1990; Kay et al., 1993; Yogodzinski et al., 1995; Stern & Killian, 1996; Rapp et al., 1999; Kelemen et al., 2003). Andesites and dacites thought to have formed by this mechanism have unusual trace element characteristics, including high Sr (>800 ppm), Sr/Y (>30), La/Yb (>10), and low Yb (<1.5 ppm) and Y (<20 ppm) compared to common island arc lavas of intermediate composition. The geochemically distinctive class of andesites and dacites with these features, now commonly termed 'adakites'

(Defant & Drummond, 1990), were first recognized by Kay (1978) who argued that they were formed through a two-step process that involved melting of the subducting oceanic crust in the presence of garnet (to produce the highly fractionated trace element patterns), followed by the interaction of the resulting silicic melt with peridotite in the hot wedge (to form the andesitic and high Mg# characteristics).

This model has been relatively successful in explaining the genesis of adakitic lavas in island arcs or other arc settings where the crust is relatively thin (e.g., Aleutians, Patagonia, Baja, Nicaragua, Panama). Recently however, the model has been applied in areas of thickened continental crust, where the mineral garnet, which plays the central role in generating the highly fractionated trace element patterns seen in adakites (Kay, 1978; Rapp et al., 1999), may be stable not only in the subducting oceanic plate, but also in the deep crust (e.g., Gutscher et al., 2000a; Beate et al., 2001; Bourdon et al., 2002; Bourdon et al., 2003). Not surprisingly, studies in this geologic setting, in particular in Ecuador, have produced a split of opinions, with some focusing on the crust as a major source of northern Andean magmatism (Kilian & Pichler, 1989; Arculus *et al.*, 1999; Monzier *et al.*, 1999), and others advocating processes within the subducting plate and mantle wedge (Barragan et al., 1998; Gutscher et al., 1999a; Bourdon et al., 2002; Bourdon et al., 2003). Reconciliation of this issue will ultimately determine the extent to which we view widespread andesite-dacite volcanism in the northern Andes as juvenile additions to the continental crust versus the recycling of old crust via intra-crustal differentiation. We therefore present in this paper whole-rock geochemical data, including Pb, Sr, and Nd isotope ratios, for Holocene and Late Pleistocene lavas collected

from the full length and width of the volcanic arc in Ecuador. The objective of this paper is to provide basic constraints on lava source, with an emphasis on improving our understanding of the contributions of crustal rocks, which in surface exposures vary from primitive oceanic terranes to evolved and geochemically mature continental lithologies.

GEOLOGIC SETTING

The spatial distribution of active volcanism in the northern Andes, which is controlled by the convergence of the Nazca and South American plates, undergoes a dramatic series of along-strike changes from central Colombia southward into northern Peru (Fig 1). In Colombia, the arc is a relatively narrow volcanic chain (40-50 km wide), which is underlain by subducting oceanic lithosphere that appears, on the basis of seismic and tomographic data, to be subducting at an angle of approximately 50° (van der Hilst & Mann, 1994; Gutscher et al., 1999a; Gutscher et al., 2000b). In the vicinity of the Columbia-Ecuador border, the volcanic arc widens abruptly (Fig. 1), and the geometry of the subducting plate becomes poorly defined by seismicity (Gutscher et al., 1999a). Further south, in central Ecuador, active volcanism terminates abruptly at Sangay Volcano, and further south again, the subduction zone enters the non-volcanic/flat-slab region in Peru (Barazangi & Isacks, 1976). The abrupt widening of the volcanic arc and the southward cessation of active volcanism in Ecuador coincides spatially with the impingement of the Carnegie Ridge on the South American margin (Fig. 1). This suggests that the deep structure of the subducting Carnegie Ridge exerts an underlying control over the surface expression of active volcanism in the Northern Andes, and plays some role in the genesis of flat-slab subduction which continues southward in Peru (Gutscher et al., 1999a; Gutscher et al., 1999b).

The north Andean crust that underlies the modern volcanoes in Colombia and Ecuador varies systematically across the margin with respect to thickness, age, rock type and geochemical maturity (Fig. 2). Estimates based on gravity indicate that crustal thickness across Ecuador changes from 25-30 km beneath the volcanic front, to more-than 50 km beneath the Inter-Andean graben and high Andes, with progressive thinning of the basement eastward toward the craton (Feininger & Seguin, 1983). In Colombia, gravity data indicates that the crust is 45-50 km thick along the axis of the Andes and that it thins to 32-35 km toward the craton and the coast (Salvador, 1991).

The geologic settings of individual volcanoes in Ecuador can be divided into three cross-arc zones, based on their distance from the trench and on the age, composition, and thickness of the crust upon-which they were built (Fig. 2). We refer to these zones (1) the volcanic-front, which lies 260-300 km from the trench, (2) the center-arc, which encompasses the Inter-Andean Graben and lies 300-380 km from the trench, and (3) the back-arc area, which lies approximately 400 km from the trench. Surface exposures of crust at the volcanic-front are composed primarily of geochemically primitive oceanic basalts and volcanoclastic rocks that were accreted to the northern Andean margin since the mid Cretaceous (Fig. 2 - Feininger, 1987; Hughes & Pilatasig, 2002). To the east, the crust beneath the center-arc becomes progressively older on average, and geochemically more mature, consisting increasingly of granites, schists, and gneisses of mostly late Mesozoic to Paleozoic age (Fig. 2 - Litherland *et al.*, 1994; Noble *et al.*, 1997). Beneath the back-arc of Ecuador, the volcanoes appear to lie above Precambrian basement at the

edge of the Brazilian shield (Precambrian rocks are absent in surface exposures, but have been recovered in cuttings from deep oil wells - Feininger, 1987). These cross-arc variations in crustal thickness/composition and geology provide a powerful basis for evaluating the potential role of crustal melting/assimilation in the genesis of lavas from volcanoes in Ecuador.

ANALYTICAL METHODS

Whole rock major and trace element concentrations were determined from fresh samples that were crushed in a steel jaw crusher and ground in agate or Al-ceramic containers. Major elements and some trace elements (Ni, Cr, Cu, V) were determined by XRF at the Washington State Geoanalytical Lab on a low dilution Li-tetraborate fused bead (Johnson et al., 1999). Trace elements concentrations were measured by ICP-MS, also at Washington State, using aliquots from the prepared XRF sample. Techniques for ICP-MS sample preparation, instrument operation, and calibrations are described in Lichte et al., (1987). Major element data for samples from Sumaco, Atacazo, and Antisana are from Barragan et al., (1998). Isotope ratios for Sr, Nd, and Pb were determined by TIMS at the University of North Carolina, Chapel Hill. All samples were dissolved at the University of South Carolina in high-purity HNO_3 and HF for three days in steel-jacketed Teflon capsules in an oven at 155° C. Chemical separates of Sr and Nd were made from the aliquoted sample by cation exchange using Sr-spec and HDEP-coated Teflon cation-exchange resins. Lead was separated by anion exchange using HBr. The Sr and Nd data are normalized to $^{86}Sr/^{88}Sr = 0.1194$ and $^{146}Nd/^{144}Nd = 0.7219$ respectively, assuming exponential fractionation behavior. The Pb data are corrected for 0.12%/amu fractionation. Reported errors in Sr and Nd data are internal run precision only. Reported

errors in Pb data are dominated by fractionation uncertainty of 0.06%/amu. All errors are 2-sigma, absolute errors. Epsilon Nd(0) is calculated with $^{143}Nd/^{144}NdCHUR = 0.512638$. For $^{143}Nd/^{144}Nd$, 20 runs of JNdi-Shin Etsu yielded a standard of 0.512110 +/- 0.000016. For $^{87}Sr/^{86}Sr$, 72 runs of NBS-987 yielded a standard of 0.710263 +/- 0.000009.

RESULTS

Basalts and Basaltic Andesites (Sumaco)

Basalts and basaltic-andesites are rare in the northern Andes, occurring in significant numbers only at Sumaco Volcano (43-54 wt% SiO_2, Table 1, Fig. 3), located in the back-arc of Ecuador (Fig. 2) approximately 400 km from the trench (Beate et al., 2001; Bourdon et al., 2003). Sumaco lavas are absarokitic and shoshonitic (1.05-4.12 wt% K_2O, Fig. 3) with silica-undersaturated compositions (Pichler et al., 1976) and incompatible trace element abundances (Rb >97, Ba >1400, Ce>170, Sr>2500 ppm; Fig. 4) that commonly lie well above those of normal subduction lavas (see also Barragan et al., 1998; Bourdon et al., 2003). Basalts and basaltic andesites from Sumaco have strongly fractionated rare-earth element (REE) patterns (La/Yb=31-43, Fig. 5A) and high Sr/Y despite the fact that Y and heavy REE concentrations are also high (Y>37, Yb>3.7 ppm; Fig. 6A). Concentrations of high-field strength elements (HFSE) are high in an absolute sense (Nb>35 ppm, Fig. 4), but are sometimes low compared to similarly incompatible large-ion-lithophile elements (LILE). This is illustrated in ratios such as Rb/Ta and Ba/Nb, which are higher than MORB at Sumaco but not as high as typical arc lavas (Fig, 7). These incompatible element ratios appear to indicate that Sumaco lavas contain a relatively small subduction-related geochemical component compared to that

which is present in the andesites and dacites that typify volcanism throughout Ecuador (Fig. 7, see also figure 4 in Barragan *et al.*, 1998).

Based on the foregoing it is clear that the lavas from Sumaco are readily distinguished from all others in Ecuador with respect to major and trace elements (Figs. 3-7). In contrast, the isotopic compositions of the Sumaco samples fall generally within the relatively narrow range of compositions observed in Ecuador (see also Harmon *et al.*, 1984; Kilian *et al.*, 1994, 1995; Barragan *et al.*, 1998; Bourdon *et al.*, 2003). The three samples from Sumaco that we have measured have isotope ratios for both Sr ($^{87}Sr/^{86}Sr$=0.7042-0.7044) and Nd ($^{143}Nd/^{144}Nd$=0.51288-0.51292) that fall near the middle-to-high end of the range of values that we report for lavas of all compositions ($^{87}Sr/^{86}Sr$=0.7040-0.7045; $^{143}Nd/^{144}Nd$=0.51273-0.51295, Table 2 and Fig. 8). In contrast, the Pb isotopes at Sumaco are relatively non-radiogenic ($^{206}Pb/^{204}Pb$=18.792-18.872; $^{207}Pb/^{204}Pb$=15.581-15.602) and fall within the field of Galapagos basalts, at the low end of a nearly vertical array of Ecuador data on plots of $^{207}Pb/^{204}Pb$ versus $^{206}Pb/^{204}Pb$, that spans the compositional range from the Galapagos Plume to average upper crust and/or local basement rocks in Ecuador (Fig. 9).

Andesite and Dacites

Medium-K, calc-alkaline andesites and dacites (SiO_2=55.76-65.98%, FeO*/MgO=1.39-1.76) are the predominant magma types erupted in Ecuador (Table 1, Fig. 3). Major element contents of MgO (2.00-6.40 wt%), CaO (4.53-7.80 wt%), FeO* (3.51-7.75wt%) and Na_2O (3.18-4.68 wt%) all show strong, linearly increasing/decreasing trends when plotted against SiO_2 (Fig. 3). In contrast, K_2O (0.87-2.99 wt%) is variable by more than a

factor-of-two across the andesite-dacite compositional range and shows only a broad, systematic increase with increasing SiO_2 (Fig. 3).

Strongly incompatible trace elements in the andesites and dacites (Rb, Ba, Ta, Nb, La, etc.) are generally correlated with one-another (Fig. 7), but like K_2O, are not well correlated with major elements indicators of crystal fractionation such as SiO_2 or MgO, (e.g., Fig. 4). Strontium (Sr) and Y, which typically exhibit moderately incompatible behavior in subduction lavas, are highly variable in abundance (Sr = 450-1200 ppm; Y = 9-23 ppm), but show no clear relationship when plotted against strongly incompatible elements such as Cs, Rb or Ba (Table 1). Strontium is similarly uncorrelated with SiO_2 but does decrease systematically with decreasing Mg# (Fig. 6B). Yttrium (Y), which is relatively low in abundance in most samples (commonly<15 ppm), generally decreases with increasing SiO_2 between 56% and 64% SiO_2, indicating that it has behaved as a moderately compatible element during the evolution of these lavas (see also figure 11 in Monzier *et al.*, 1999). Strongly compatible trace elements such as Cr and Ni, are highly variable in the andesites and dacites(Cr up to 240 ppm) and like many of the most incompatible elements, also appear to be largely independent of SiO_2 (e.g., Fig. 4).

Ratios among the incompatible elements in andesites and dacites are clearly characteristic of a subduction zone setting and in most ways are typical of andesites and dacites throughout the Andes. Ratios of LILE's to HFSE's (e.g., Rb/Ta, Ba/Nb) are elevated across-the-board in the andesites and dacites compared to oceanic basalts (Fig. 7). The REE are highly variable with regard to both elemental abundance and pattern shape (Fig.

5). The total range for La/Yb is high (4.3-38.8, Table 1), but there is a strong clustering of samples at relatively low La/Yb (6-10) and progressively fewer samples with more highly fractionated patterns (only 4 samples with La/Yb>20 – Fig. 10). Among the samples with La/Yb>10, some are clearly depleted in the heavy REE's (Yb<1.0) and have fractionated heavy REE patterns with normalized Dy/Yb>2.0, whereas others are primarily enriched in the light REE's and have obviously flatter heavy REE patterns (Fig. 5A). The most common andesites and dacites have straight and modestly fractionated patterns with La/Yb = 6-10 and normalized Dy/Yb<2.0 (Fig. 5B). Overall, these REE characteristics do not stand out as unusual compared to andesites and dacites from other parts of the Andes (Fig. 10). Relative Ba concentrations are also variable and high in andesites and dacites (Ba/La=20-80), and in this way the Ecuador lavas are similar to lavas in island arcs but are unlike andesites and dacites of the central and southern Andes which typically have Ba/La<25 (Fig. 11 - Hildreth & Moorbath, 1988; Davidson *et al.*, 1990). In addition, nearly all of the andesites and dacites from Ecuador have high Sr/Y (22-70, Fig. 6A), and according to the criteria of Defant and Drummond (1990), most would be classified as adakites (see also Beate et al., 2001; Bourdon et al., 2002; Samaniego et al., 2002; Bourdon et al., 2003). In this regard, the rocks from Ecuador are also typical of andesites and dacites from throughout the Andes (Figs. 6, 10).

Trace element characteristics in andesites and dacites also change systematically west-to-east across the magmatic arc in Ecuador. In general, the average incompatible element concentrations are higher in the center arc and back-arc areas, at greater distances from the trench (Fig. 11A, B). Certain incompatible element ratios, for example Ba/Nb and

La/Yb, also change systematically across the arc (Fig. 11C, D - see also Hörmann & Pichler, 1982; Kilian & Pichler, 1989; Vanek *et al.*, 1994; Barragan *et al.*, 1998). These patterns are similar to those seen in magmatic arcs worldwide (Dickinson, 1975).

Isotopically, andesites and dacites from Ecuador define a relatively narrow range of values that fall within the Sr-Nd mantle array and overlap somewhat with Galapagos plume basalts for each of the isotopic systems studied (Sr, Nd, Pb – Figs. 8-9). Isotope ratios for Sr and Nd that we report ($^{87}Sr/^{86}Sr$=0.7040-0.7044, $^{143}Nd/^{144}Nd$=0.51273-0.51295; Table 2) lie at the primitive end of the field of modern Andean lavas (Fig. 8) and encompass nearly the full range of published values for the northern volcanic zone (Harmon *et al.*, 1984; Kilian *et al.*, 1995; Barragan *et al.*, 1998; Bourdon *et al.*, 2003). For Pb isotopes, the andesites and dacites, as described above, form a near-vertical trend on plots of $^{207}Pb/^{204}Pb$ versus $^{206}Pb/^{204}Pb$, spanning the compositional gap between Galapagos basalts and average upper crust and/or local basement (Fig. 9). The data from Ecuador are broadly like those from Colombia (James & Murcia, 1984), but contrast sharply with Pb isotope ratios in lavas of the central and southern Andes, which commonly have $^{206}Pb/^{204}Pb$ values that are low (approaching Precambrian basement in Peru), resulting in a nearly horizontal data array in $^{207}Pb/^{204}Pb$ versus $^{206}Pb/^{204}Pb$ graphs (Fig. 9). It is convenient to quantify Pb isotope variation in Andean lavas in terms of Δ7/4 Pb, which is a quantitative expression of deviation in $^{207}Pb/^{204}Pb$ away from the mantle reference line at the $^{206}Pb/^{204}Pb$ composition of the sample (Hart, 1984). Expressed in this way, Pb isotopes in Ecuador andesites and dacites are inversely correlated with Nd isotopes, and appear to fall along mixing lines between Galapagos

plume basalts and average upper crust and/or local, geochemically evolved basement rocks in Ecuador (Fig. 12).

Isotopic compositions of andesites and dacites also change east-to-west across the magmatic arc in Ecuador and in response to changes in certain trace element parameters. Specifically, $^{87}Sr/^{86}Sr$ and $\Delta 7/4$ Pb in the Ecuador lavas reach their highest values in lavas erupted in the center-arc region (330-360 km from the trench), along the crest of the Andes where the crust is likely to be thickest (Fig. 13). Conversely, $^{143}Nd/^{144}Nd$ is lowest across this region (Note however, that the alkaline basalts and basaltic andesites from Sumaco Volcano in the back-arc area do not follow the cross-arc istopic patterns of the andesites and dacites – Fig. 13). Isotopic compositions of andesites and dacites in Ecuador also change systematically with increasing incompatible element concentrations (e.g., decreasing $^{143}Nd/^{144}Nd$ with increasing Nb, Ba, Rb, La – Fig. 14), and with changes in certain trace element ratios, especially Ba/Nb and La/Yb, and to a lesser extent Ba/La (Fig. 15). In general, the trace element - isotope relationships are clearest when they involve the Nd and Pb isotope ratios, but are absent or less clear when they involve either Sr or $^{87}Sr/^{86}Sr$. Finally, there appears to be no clear systematic relationship between any of the isotopic systems and any major element parameter in the andesite-dacite compositional range (Fig. 16).

Rhyolites

Rhyolites reported here are from Chacana, Chalupas, and Cotopaxi volcanoes, which are all located in the center-arc area, around the Inter-Andean Graben, along the crest of the Andes in northern Ecuador (Table 1, Figs. 1-2). Aside from the obvious gap in silica

between approximately 66% and 71% SiO_2 (evident on Harker-type diagrams – Fig. 3) the major and trace element compositions of the rhyolites from Ecuador appear in a broad sense, to be extensions of the andesite-dacite compositional trends (Figs. 3-5). One exception is in the REE patterns, which are clearly flatter in the heavy REE's (normalized Dy/Yb<1.50) and have 18-57% negative Eu anomalies (i.e., Eu/Eu*=0.43-0.82, Fig. 5C). The broad similarity with respect to trace elements does not extend to the isotopic compositions, which on-average, are more radiogenic in Pb and Sr and less radiogenic in Nd in the rhyolites compared to the andesites and dacites (Figs. 8, 9, 13, 14, 15). This is essentially as-expected of high-SiO_2 melts containing a somewhat higher proportion of geochemically evolved crust rock relative to mantle components.

DISCUSSION

Isotopic Constraints on Crustal Components in Ecuador Lavas

Compared to the central and southern Andes, where the case for substantial melting and assimilation of geochemically evolved crustal rock has been well documented (e.g., Hildreth & Moorbath, 1988; Davidson et al., 1990; Kay & Kay, 1991), lavas in Ecuador fall within a narrow range of relatively primitive isotopic compositions, overlapping somewhat with Galapagos Plume basalts for $\Delta 7/4P$, $^{87}Sr/^{86}Sr$ and $^{143}Nd/^{144}Nd$ (Figs. 8-9). Isotopic compositions in Ecuador lavas are also appear to be largely independent of major element composition (Fig. 16) and of the age and composition of the crust through which they erupted (e.g., compare back-arc and volcanic front in Fig. 13). This is particularly evident for the lavas from Sumaco, which are mafic and alkaline in composition (nepheline-normative), and appear to have erupted through geochemically

mature Precambrian crust, but have Sr and Nd isotope ratios that overlap broadly with the common sub-alkaline andesites and dacites at the volcanic-front, where the volcanoes are underlain by geochemically immature oceanic terranes of Mesozoic age (Fig. 13). These observations, which clearly indicate a limited role for geochemically mature continental crust in the genesis of modern lavas in Ecuador (see also Harmon *et al.*, 1984; James & Murcia, 1984), are supported by certain trace element ratios, especially Ba/La, which is variable and high in Ecuador lavas (similar to island arc basalts) and in this way unlike lavas of the central and southern Andes where Ba/La is, apparently because the lavas there have assimilated large quantities of granitic crust (Fig. 11 - Hildreth & Moorbath, 1988; Davidson *et al.*, 1990).

Arculus et al. (1999) pointed out that melts extracted from a garnet-bearing mafic lower crust might be in-part, the source of the adakitic trace element patterns and relatively non-radiogenic isotopes observed in Ecuador andesites and dacites (see also Kilian *et al.*, 1994, 1995; Monzier *et al.*, 1999). However, recently published isotopic data appear to rule out the oceanic terranes as a viable source for the modern lavas in Ecuador. This is true primarily because of the Pb isotope ratios, which are highly variable and relatively non-radiogenic in the oceanic terranes, with low $^{206}Pb/^{204}Pb$ and $^{207}Pb/^{204}Pb$ compositions that clearly contrast with those observed in Ecuador lavas (Fig. 9). More broadly, geophysical and geological observations lead us to conclude that the oceanic terranes that underlie western Ecuador are unlikely to be present beneath the volcanoes in central Ecuador at depths where garnet would be stable and crustal melting might produce fractionated trace element patterns (high La/Yb, Sr/Y) such as those observed the modern

lavas. In particular, gravity anomalies to positive 162 mgals over the volcanic-front of Ecuador and negative 292 mgals at the center of the volcanic arc seem to require a major change in crustal lithology and thickness separating these two segments (Feininger & Seguin, 1983). In addition, seismic, gravity and structural data indicate that oceanic terranes in Colombia, just north of Ecuador, were emplaced along low-angle thrusts and are therefore no more than 10-15 km thick and are underlain by relatively low-density (i.e., 'normal') rock in the middle and deep crust (Kellogg & Vega, 1995). We therefore infer from geophysical constraints that the terrane boundaries in Ecuador are not near-vertical structures (as indicated in figure 1 of Kilian *et al.*, 1994), and that the oceanic terranes that underlie western Ecuador do not extend to significant depths beneath the volcanoes in central and eastern Ecuador -- a feature that would be required if they were to play a significant role in the genesis of 'adakitic' andesite and dacites lavas in the area.

Based on the foregoing it appears that the isotopic data rule out wholesale melting of crustal rocks (similar to those that are exposed at the surface in Ecuador), as a major source for the andesite and dacite lavas there. It remains possible of course, based on isotopic data alone, that melts from newly underplated mafic crust (formed in the modern subduction zone and therefore isotopically similar to the modern lavas), could have contributed significantly to the source of the Ecuador lavas. Such an origin, which involves rapid remelting of recently created (i.e., newly underplated) basaltic deep crust, has been proposed in Ecuador (Monzier *et al.*, 1999) and in other areas of thickened crust in the Andes, in particular in the case of the Miocene Cordillera Blanca Batholith in Peru (Petford & Atherton, 1996). At some level, this process seems inevitable in any

vigorously active magmatic arc. It is however, unlikely that this process has exerted a major influence on magma genesis in the modern volcanic arc Ecuador, where the lavas are mostly medium-K, calc-alkaline andesites which clearly contrast in major element composition, the dominantly silicic, alkali-rich and leucocratic granites that dominate the Cordillera Blanco location in Peru (SiO_2 >70%, Na_2O>4% K_2O>3%, MgO<2%, FeO*<2%) that appear to have formed by a regional-scale, crustal melting event during the Miocene (Petford & Atherton, 1996). Felsic melts of this broad major element type in Ecuador are present in the rhyolites, but they are a relatively small proportion of what has erupted at the surface, and unlike leucogranites from the Cordillera Blanco, the Ecuador rhyolites have relatively flat heavy REE patterns and do not possess the kinds of highly fractionated trace element patterns that contrast strongly with associated rocks of more mafic-and-intermediate compositions (e.g., compare figure X here with figure 9 in Petford & Atherton, 1996).

Having emphasized that crustal rocks of the northern Andes have played a limited role in the genesis of Ecuador lavas compared to other parts of Andes where assimilation and wholesale melting of the crust appears to be common, it is important to point out that the isotope systematics clearly indicate that, similar to the case in Colombia (James & Murcia, 1984) at least some assimilation of continental crust has affected many of the samples from Ecuador that we have analyzed. This is particularly clear from Pb and Nd isotope data, which are well correlated and appear to define mixing lines between Galapagos Plume / Carnegie Ridge basalts (i.e., probable subducting plate and mantle wedge compositions) and the local, geochemically mature crustal rocks that underlie the

volcanoes in central Ecuador (i.e., probable assimilants – Fig. 12). Bulk mixing calculations along this Pb-Nd correlation indicate that most lavas in Ecuador contain no more than 5-10% of the local, geochemically mature crustal rock (Fig. 12). Incorporation of this material into the Ecuador lavas by the process of assimilation is well supported by observed spatial-geochemical shifts in isotopic compositions across that arc, which reach maximum values for $^{87}Sr/^{86}Sr$ and $\Delta 7/4Pb$, and minimum values for $^{143}Nd/^{144}Nd$, over the crest of the northern Andes, in the area around the Inter-Andean depression, at distances of 330-360 km from the trench (Fig. 13). Based on the high elevations and on the presence of rhyolitic volcanism at Cotapaxi, Chalupas and Chacana, this area, around the Inter-Andean depression, appears to be the part of the Northern Andes where the crust is thickest, warmest and weakest, and where it is therefore most likely to contribute as an assimilant to melts in-transit from the subduction zone to the surface (see also geophysical arguments in Salvador & Kellogg, 1991).

Our estimate of crustal contamination in Ecuador lavas, which is somewhat lower than some previous estimates (Kilian *et al.*, 1995; Barragan *et al.*, 1998), assumes that the entire shift in correlated Pb and Nd isotopes (away from Galapagos basalts and toward geochemically mature upper crust in Ecuador – Fig. 12) is attributable to crustal assimilation and that none is due to either subduction erosion along the plate boundary (a likely response to Carnegie Ridge subduction beneath Ecuador - e.g., von Huene & Scholl, 1991) or to the subduction of continentally derived marine sediment into the mantle wedge (a process that is well documented in island arcs, and should therefore also be common in continental subduction systems e.g., Kay et al., 1978 ; Morris et al., 1990;

Plank & Langmuir, 1993). If, as seems likely, these processes have played a role in controlling the isotopic compositions of melts formed in the subduction zone beneath Ecuador, then our already-low estimate of the crustal contributions to these lavas would have to be revised downward (see also James, 1982).

According to this interpretation, a significant proportion of the Ecuador lavas have remained unaffected or minimally effected by assimilation of geochemically mature continental crust (e.g., samples with $\Delta 7/4Pb < 6.80$ and $\varepsilon Nd > 4.0$ – Figs. 8-9). We cannot of course, rule out the possibility that all of our lavas have been greatly affected by crustal assimilation, and that isotopically more primitive parental magmas are never erupted at the surface and therefore have not been sampled. We do not believe this is the case for two reasons. First, a large number of the Ecuador andesites and dacites have Pb, Sr and Nd isotopic compositions that are tightly clustered and approach and overlap-with likely subducting plate compositions in the form of Galapagos Plume and Carnegie Ridge basalts. This is effectively the same as the situation in many island arcs where the Pb, Nd and Sr isotopic compositions of the lavas approach those of MORB and are therefore widely believed to be controlled primarily by the composition of the subducting plate in the form of seawater-altered MORB + sediment (Kay, 1980; Plank & Langmuir, 1993; Elliott et al., 1997; Class et al., 2000). Second, the alkaline basalts and basaltic andesites at Sumaco, which appear, based on major and trace element compositions to be low-percentage melts of mantle peridotite which has been only modestly affected by subduction metasomatism (Barragan et al., 1998; Bourdon et al., 2003), have extraordinarily high concentrations of Pb, Sr and Nd, which would have caused these

melts to be much more resistant to isotopic shifts during crustal assimilation than would the andesites and dacites which have lower concentrations of these elements and are generally more evolved (lower Mg#) and were probably erupted at lower temperatures. Assuming that more silicic and cooler lavas are more likely to have assimilated crust on their way to the surface (DePaolo, 1981), the broad isotopic overlap between the mafic alkaline lavas at Sumaco and the andesites and dacites clearly suggests that control over the isotopic composition of Ecuador melts lies primarily is in the subduction zone and not in the continental crust through-which the melts passed.

Effects of Crustal Assimilation on Trace Elements

Based on the prior discussion, it should be clear that formation of the andesites and dacites in Ecuador, which are nearly all adakites based on the criteria of Defant and Drummond (1990) and Drummond et al., (1990), was not by wholesale melting or extensive assimilation of the continental crust, but that many of these lavas nonetheless assimilated a measurable quantity of geochemically mature crustal rock prior to their eruption. This raises the obvious question: What role, if any, has crustal assimilation played in producing, enhancing or altering the adakitic trace element features of andesites and dacites in Ecuador?

Ecuador andesites and dacites that have relatively high $\Delta 7/4Pb$, $^{87}Sr/^{86}Sr$ and low $^{143}Nd/^{144}Nd$ (i.e., those that appear to have assimilated a significant quantity of continental crust), generally have more variable and higher concentrations of the most incompatible trace elements, including Rb, Cs, Nb, Zr, Ba, Pb, and La (Fig. 14). For

example, among the andesites and dacites with $^{143}Nd/^{144}Nd<0.51285$ ($\varepsilon Nd<4.1$), four samples of five have Zr>100 ppm, whereas none with $^{143}Nd/^{144}Nd>0.51285$ have Zr>100 ppm. A similar relationship can be seen in the Nb concentrations, which show a clear inverse correlation with $^{143}Nd/^{144}Nd$, but not for Y or Yb, where the elemental concentration appears to be independent of isotope ratios (Fig. 14). Not surprisingly, the rhyolites generally also have elevated concentrations of the strongly incompatible elements and concomitantly higher $^{87}Sr/^{86}Sr$ and $\Delta 7/4Pb$, and lower $^{143}Nd/^{144}Nd$, consistent with (on average) a relatively higher proportion of crustal rock in the cooler and silicic and more evolved rhyolitic melts (Fig. 14). Similar systematics can be seen in most graphs of isotope ratios plotted against incompatible element concentrations, however most of these correlations are relatively weak, and it is commonly true that nearly the full range of isotopic compositions is present in samples at all incompatible element abundance levels (e.g., Ba, Sr, and Y in Fig. 14).

Isotopic shifts attributable to crustal contamination are also accompanied by shifts in certain incompatible element ratios. This is particularly clear for La/Yb, which is generally higher, and for Ba/La and Ba/Nb, which are generally lower in samples with relatively low $^{143}Nd/^{144}Nd$ and high $^{87}Sr/^{86}Sr$ (i.e., those that appear to have assimilated continental crust Fig. 15). These relationships imply that cross-arc changes in La/Yb, Ba/Nb, etc., for the andesites and dacites is produced by assimilation of thickened and warmed continental crust, and not (as has been consistently argued in the literature) by increased depth and/or percentage melting or by decrease slab-fluid input to the mantle wedge. We do not apply this interpretation to the back-arc mafic and alkaline lavas at

Sumaco, which anchor the cross-arc trends with high La/Yb and low Ba/Nb, but also retain the high $^{143}Nd/^{144}Nd$ and low Δ7/4Pb that is characteristic of lavas at the volcanic front (Fig. 13). We agree with the interpretation of the Sumaco lavas as deep, low-percentage melts of mantle peridotite (Barragan *et al.*, 1998; Bourdon *et al.*, 2003), but as-such, we view their genesis as fundamentally distinct from the subalkaline andesites, dacites and rhyolites that dominate volcanism in Ecuador.

In contrast to La/Yb and Ba/Nb, which appear to be significantly affected by crustal assimilation, the full range of Sr/Y observed in the Ecuador Andesites and dacites appears to be present among samples with relatively primitive isotopic composition (e.g., $^{143}Nd/^{144}Nd>0.51285$, Δ7/4 Pb<7.0, Fig. 15). This suggests that Sr/Y, a key ratio in the adakite characterization, is not substantially affected by crustal assimilation in andesite and dacite lavas in Ecuador. To the contrary in fact, data from individual volcanoes where significant crustal assimilation has occurred and where several andesite and dacite samples have been analyzed (e.g., Antisana, Imbabura) Sr/Y and Sr concentration appear to be inversely correlated with Δ7/4Pb, suggesting that these quantities are highest in the samples that have assimilated the least amount of continental crust (Fig. 17). This is one of the few geochemical parameters, along with Ba/La, that appears to distinguish andesite and dacite lavas in Ecuador from those in the central and southern Andes (Figs. 11, 18).

We conclude that crustal assimilation has systematically changed the trace element character of some Ecuador lavas, especially those from the center-arc area, around the Inter-Andean depression. It is also clear that some of the most adakitic andesites and

dacites that we have analyzed (e.g., with La/Yb>20) are those that appear, on the basis of their isotopes, to have assimilated the most crust. There is, nonetheless, a well defined subset of andesite samples from Ecuador that has geochemical features (including Sr>900 ppm and relatively non-radiogenic isotopes), consistent with an origin by melting of subducting oceanic crust at high pressures and in the presence of garnet (i.e., the adakite model of Kay, 1978; Defant & Drummond, 1990).

Origin of the Adakite Trace Element Pattern & Role of the Carnegie Ridge

Cenozoic igneous rocks with adakitic trace element patterns occur in a variety of settings and have been interpreted to have formed by a variety of processes including (1) melting of subducting oceanic lithosphere, commonly referred to as 'slab melting' (e.g., Kay, 1978; Saunders et al., 1987; Defant & Drummond, 1990; Kay et al., 1993; Stern & Killian, 1996; Kepezhinskas et al., 1997), (2) melting of garnet-bearing deep crust, especially in continental settings where the crust is unusually thick (e.g., Kay & Kay, 1991; Petford & Atherton, 1996), and (3) crystal fractionation processes involving amphibole and/or garnet or other minerals capable of increasing La/Yb and Sr/Y in evolved melts (e.g., Castillo et al., 1999; Garrison & Davidson, 2003). Based on the isotopic data discussed previously, wholesale melting of a garnet-bearing deep crust beneath the Northern Andes and/or large-scale assimilation of such crust appear to be unlikely scenarios for producing the ubiquitous adakitic characteristics of andesite and dacite lavas in Ecuador. This leaves the slab-melting and crystal fractionation processes for us to consider.

In island arcs and other settings where the crust is relatively thin, the slab-melt interpretation hinges on the observation that the adakitic trace element pattern is most strongly developed in primitive lavas, commonly magnesian andesites, which have relatively high whole-rock Mg# and elevated Cr and Ni contents, consistent with a mantle origin (i.e., the rocks with the highest Sr/Y, La/Yb and $^{143}Nd/^{144}Nd$ are observed in the most primitive lavas which are andesites – not basalts). It was the combination of fractionated trace element patterns (high La/Yb, Sr/Y) with MORB-like isotopes and Mg-rich andesitic major element and mineralogic characteristics that lead Kay (1978) and have lead most subsequent workers, to interpret primitive adakitic lavas from the Aleutians, Baja, Patagonia, and elsewhere, as silicic melts of subducting oceanic crust that were extracted from a garnet-bearing residue and subsequently interacted with mantle peridotite to produce a primitive magnesian andesite (Kay, 1978; Rogers et al., 1985; Saunders et al., 1987; Yogodzinski et al., 1995; Stern & Killian, 1996). The evolution of such magnesian andesite melts, by crystal fractionation and/or mixing with 'normal' calc-alkaline magmas, has been used to explain the geochemistry of all adakitic lavas in these areas, including the dacitic varieties with low Mg# (similar to many Ecuador lavas) and only modest geochemical enrichments over 'normal' calc-alkaline lavas (Stern & Killian, 1996; Yogodzinski & Kelemen, 1998). In these cases, the primitive end-member was the smoking gun and the slab-melt interpretation (for the evolved and more geochemically ambiguous samples) was largely by association.

In Ecuador, there are no exceptionally primitive lavas (i.e., none with Mg#>0.65), and therefore no clear link between the adakite trace element pattern and lavas that are

obviously mantle-derived. Moreover, it seems clear that crystal fractionation has significantly affected certain trace elements that play a central role in the adakite characterization. In particular the decrease in Y concentration with increasing SiO_2, which is evident in our data from all centers (Fig. 4), but is more clearly illustrated in data from individual centers where several data points are available (e.g., figure 11 in Monzier *et al.*, 1999), seems to imply that Y commonly behaves as an compatible element in the andesite-dacite compositional range in Ecuador. It is possible, perhaps likely, that this behavior is in response to crystal fractionation of amphibole, which is a common phenocryst phase in Ecuador lavas, or possibly garnet, which has not been observed in the lavas but may be been stabilized in andesites and dacites under deep, high-pressure conditions (Stern & Wyllie, 1978). The alternative interpretation of the Y-SiO_2 relationship would involve mixing between mafic melts of the mantle (low SiO_2 and high Y) and silicic melts of amphibole or garnet-bearing deep crustal rock (high SiO_2 / low Y), but this process seems unlikely based on the isotopic data discussed at length above.

Evidence for crystal fractionation effects on Y and Yb concentrations in andesites and dacites in Ecuador was also presented by Samaniego (2002), who documented a stratigraphic succession from older, amphibole-free calc-alkaline lavas at Cayambe Volcano with relatively high Y and Yb abundances, to an overlying / younger set of amphibole-bearing adakitic lavas with low Y and Yb. The presence of amphibole phenocrysts in the adakitic lavas (Y<12 ppm, Yb<1.0 ppm), and the absence of amphibole from the calc-alkaline lavas (Y>15ppm, Yb>1.0 ppm) is consistent with the

idea, discussed by Castillo et al., (1999) and Garrison and Davison (2003), that amphibole fractionation may produce high Sr/Y and low Y, especially under high water pressures which suppress plagioclase crystallization and thereby allow Sr concentrations to increase or remain high as the melts evolve (i.e., a crystal fractionation process that drive melts up-and to-the-left on plots of Sr/Y versus Y). Based on the clear inverse relationship between Y concentration and SiO_2 in the andesite-dacite compositional range (Fig. 3), it seems certain that crystal fractionation of amphibole and perhaps garnet have played a role in controlling the trace element patterns in many (perhaps most) lavas in Ecuador (e.g., Samaniego et al., 2002; Garrison & Davidson, 2003). This implies in-turn that interpretations of adakite geochemistry in island arc lavas cannot be applied in a straightforward way to volcanic rocks in Ecuador or other areas of thick crust where Y and Yb are not reliably incompatible elements, and where high Sr/Y and La/Yb have therefore been, to varying and unknown degrees, affected by crystal fractionation.

It is equally clear however, that some of the lavas in Ecuador, in particular those with >900 ppm Sr, define a distinctive high-Sr group that appears unlikely to have been produced by crystal fractionation and assimilation based on their Sr - Mg# relationships and their primitive isotopic compositions (Fig. 17). This geochemically distinctive group of lavas is well illustrated in our data from Imbabura Volcano where a high-Sr liquid line of decent (perhaps a mixing line) is clearly separate from the evolutionary pathway that is produced by lavas with 400-600 ppm Sr over the same range of SiO_2 and Mg# (Fig. 17). This distinctive, high-Sr and isotopically primitive geochemical type also appears to be present at Antisana Volcano (Fig. 17) and can be seen in data from Puñalica Volcano

where it defines an end-member composition with regard to both high Sr (>850 ppm) and non-radiogenic Sr isotopes ($^{87}Sr/^{87}Sr<0.7039$) among the 23 samples from the northern Andes studied by Harmon et al., (1984). This geochemical end-member, which is not abundant in Ecuador and does not appear to exist among lavas of the central and southern Andes (Fig. 17) or in Colombia (James, 1982), is the only clear candidate for a slab-melt interpretation that we see in the available data from the northern Andes. However, due to the evolved, low-Mg# nature of the lavas, it is impossible to rule out the alternative model in which Sr in these lavas is elevated to high concentrations by crystal fractionation at high water pressures and in the absence of plagioclase crystallization (e.g., Garrison & Davidson, 2003).

Beyond these observations, it seems unlikely that whole-rock data of the type and quantity that we have presented can be used to unambiguously distinguish between source and fractionation effects to explain the high-Sr and isotopically primitive lavas from Imbabura and other volcanic centers in Ecuador. Better sampling within individual volcanoes and a texturally specific / microbeam analytical approach, perhaps involving studies of melt inclusions which may capture more primitive major element compositions, will probably be required to more clearly define the important geochemical end-members involved in these systems (Yogodzinski & Kelemen, 1998; Davidson *et al.*, 2000).

Based on the foregoing it should be clear that in our view, the role of the subducting Carnegie Ridge in controlling the geochemistry of volcanic rocks in Ecuador remains

uncertain. An important consideration for future work will be a careful and systematic comparison between lavas formed above the Carnegie Ridge in Ecuador with those formed in Colombia, especially in areas well north of the landward projection of the Carnegie Ridge. It is clear that andesite and dacite lavas in Ecuador and Colombia are broadly alike with regard to most geochemical indicators including their 'adakitic' Sr/Y versus Y characteristics (e.g., Fig. 6). Based on the available isotopic data, which remains sparse in the northern Andes, we see no evidence that there exists a high-Sr (>900 ppm) and isotopically primitive geochemical end-member in modern lavas from Colombia (James & Murcia, 1984), similar to that which is clearly present in our data from Imbabura and perhaps Antisana and Puñalica (Fig. 17). If future studies fail to reveal this high-Sr end-member among modern lavas in Colombia (Sr>900 ppm; $\Delta 7/4Pb<7.0$; $\varepsilon Nd>4.0$), it will be logical to conclude that its presence in Ecuador may reflect a role for melting of the warm and over-thickened oceanic crust of the subducting Carnegie Ridge (Gutscher et al., 2000b; Bourdon et al., 2002; Bourdon et al., 2003). If such a geochemical distinction between lavas in Colombia and Ecuador can be well documented (i.e., if the isotopically primitive, high-Sr geochemical type is not present in Colombia), it will bolster the idea that the Carnegie Ridge holds some underlying control over magma genesis beneath Ecuador. If alternatively, the high-Sr, isotopically primitive lava type is eventually found among Colombian lavas, and especially if it is found in volcanoes located well north of the landward projection of the Carnegie Ridge (Fig. 1), the hypothesized role for the Carnegie Ridge in the genesis of andesite and dacite lavas in Ecuador will viewed with increasing skepticism (Garrison & Davidson, 2003).

An alternative, more historical approach to understanding the role of the Carnegie Ridge in melt genesis beneath Ecuador, similar to that which has been used to understand the role of subducting plate geometry and crustal thickening in the central Andes (Kay *et al.*, 1987; Kay *et al.*, 1988), would be through a study of the older, Neogene-age lavas which exist in a variety of places among Miocene and Oligocene strata in Ecuador (Hall & Calle, 1982). If studies of these older lavas fail to reveal the existence of isotopically primitive andesites and dacites with >900 ppm Sr, it will encourage the idea that the presence of this end-member in the modern volcanoes of Ecuador is tied to the subduction of the Carnegie Ridge (Gutscher *et al.*, 2000b; Bourdon *et al.*, 2003). Geochemical data on Neogene volcanic rocks in Ecuador are currently sparse and inconclusive on this question (Kilian *et al.*, 1995). If however, it can be shown that the Carnegie Ridge is in any significant way influencing the genesis of melts in the modern subduction zone in Ecuador, that influence could be quantified and the timing of it's arrival in the subduction zone could be determined through combined geochemical and geochronological investigations into the Neogene lavas in Ecuador. It will be only such historical investigations, coupled with more thorough characterization of intra-and-inter-volcano variation both in Ecuador and in Colombia (especially in areas well north of the landward projection of the Carnegie Ridge) that will eventually resolve the question of how, if at all, the subduction of the Carnegie Ridge has influenced magmatism and crustal growth in the modern subduction zone beneath Ecuador.

CONCLUSIONS

1. Primitive and relatively homogeneous isotopic compositions observed across the arc imply that Ecuador lavas were produced largely within the subduction zone and not by extensive melting of crustal rocks similar to those upon-which the volcanoes were built. Mixing calculations limit the quantity of assimilated crust to less than approximately 10%. These constraints are based on a limited knowledge of basement rock geochemistry, but the tight geochemical clustering of most andesite and dacite lavas in Ecuador, combined with their isotopic similarity to back-arc alkaline basalts that have trace element ratios that are transitional toward MORB and OIB, severely limit the role of crustal melting and/or assimilation in most Ecuador lavas.
2. Cross-arc geochemical variation (e.g., in $^{143}Nd/^{144}Nd$, Ba/Nb, La/Yb) indicates that assimilation of crustal rock is most active in the center-arc area, around the Inter-Andean Graben, at distances from 330-360 km from the trench, in the main area of thick and thermally weakened crust in Ecuador.
3. Characteristically 'adakitic' trace element features (low Y, Yb, high La/Yb), which are observed in virtually all andesites and dacites in Ecuador as well as throughout the central and southern Andes, are influenced to a significant degree, by crystal fractionation. This is most clearly illustrated by the compatible-element behavior for Y, which decreases systematically in with increasing SiO_2 in the andesite-dacite compositional range. Adakitic trace element features are also most strongly developed in lavas that, based on isotopic compositions, appear to have assimilated the most crust.

4. A subset of andesites display an unusual combination of high Sr (>900 ppm) and non-radiogenic isotopes ($\varepsilon Nd > 4.1$, $\Delta 7/4Pb < 6.0$) and appear to be regionally distinctive in Ecuador (i.e., not observed among modern lavas in the Andean central and southern volcanic zones or in Colombia). Only these lavas, which are well represented at Imbabura Volcano, appear to have geochemical features that may be consistent with a slab-melt interpretation associated with the subduction of relatively young, over-thickened oceanic crust of the subducting Carnegie Ridge.

FIGURE CAPTIONS

Fig. 1 Topographic and bathymetric map of the Northern Andes region, showing major geographic features mentioned in the text. Red triangles mark the locations of Quaternary volcanoes from the Smithsonian Global Volcanism database. Black arrows show the convergence direction and rate of movement of the Nazca Plate relative to stable South America from Trenkamp et al., (2002).

Fig. 2 Tectonic map of Ecuador showing locations of major terrane boundaries and types from Noble et al., (1997) and Litherland et al. (1994). Sample lavas include basalts, andesites, dacites and rhyolites from the 12 volcanoes (white triangles) across the 150-km width of the arc.

Fig. 3 Major element variation in volcanic rocks from Ecuador. All data here are from Table 1. Symbols for compositional categories defined here (basalt-basaltic andesite, andesite-dacite, rhyolite) are used throughout this paper. Calc-alkaline / tholeiitic boundary line is from Miyashiro (1974). Boundaries defining low, medium and high-K series are from Ewart (1982).

Fig. 4 Variation in trace element concentrations as a function of SiO_2 for Ecuador volcanic rocks. All shown data here are from Table 1. Symbols are as in figure 3.

Fig. 5 Rare-earth element (REE) variation in volcanic rocks from Ecuador. Examples in figure 5A have La/Yb>10 including basalt, andesite and dacite compositions. High REE concentrations and steep patterns in alkali basalt sample 3D3 (La/Yb>35) appear to be characteristic of most lavas from Sumaco Volcano (see also Barragan *et al.*, 1998; Bourdon *et al.*, 2003). Andesites from Antisana (La/Yb=38.8), Chacana (La/Yb=37.1), Quilotoa (La/Yb=16.8) and Imbabura (La/Yb=10.1) have strongly to moderately fractionated REE patterns compared to those illustrated in 5B from Atacazo (La/Yb=8.0), Chacana (La/Yb=8.6) and Imbabura (La/Yb=7.5) which are more typical in Ecuador, showing less highly fractionated REE patterns with La/Yb in the 6-10 range. Figure 5C illustrates typical rhyolite patterns showing high La/Sm, significant negative Eu anomalies and relatively flat heavy REE's with normalized Dy/Yb<1.5. Field of leucogranites illustrates the contrasting REE characteristics of the Ecuador rhyolites compared to similarly felsic leucogranites from the Cordillera Blanco Batholith, Peru. Stippled field in figures 5B-C is from the field bounded by the Antisana andesite and the Quilotoa dacite in figure 5A. Leucrogranite data are from Atherton and Petford (1993). All other data are from Table 1.

Fig. 6 Graphs of Sr/Y versus Y (6A) and Sr concentration versus Mg# (6B). Figure 6A shows the characteristically adakitic nature of virtually all andesite and dacite lavas in Ecuador and Colombia, similar to volcanic rocks throughout the Andes. Figure 6B illustrates the variably high Sr concentration at high Mg# and general inverse relationship between Sr and Mg#, again, typical of lavas throughout the Andes. Ecuador data (large symbols as in figure 3) are from Table 1. Boundaries for 'adakitic' and 'calc-alkaline' fields have been approximated from figure 15 in Defant et al., (1991). Central and southern volcanic zone data are from published sources (Lopez-Escobar *et al.*, 1977; Deruelle, 1982; Thorpe *et al.*, 1983; Frey *et al.*, 1984; Harmon *et al.*, 1984; Lopez-Escobar, 1984; Lopez-Escobar *et al.*, 1985; Hickey *et al.*, 1986; Davidson *et al.*, 1988; Futa & Stern, 1988; Hildreth & Moorbath, 1988; Wörner, 1989; Davidson *et al.*, 1990; Walker *et al.*, 1991). Colombia data are from Galeras Volcano (Calvache & Williams, 1997) and from Nevado del Ruiz (Sigurdsson *et al.*, 1990).

Fig. 7 Incompatible element concentrations and ratios in Ecuador lavas compared to MORB. Relatively MORB-like ratios (Rb/Ta, Ba/Nb, etc.) for alkali basalts and basaltic andesites from Sumaco Volcano (black squares) indicate that these lavas have a relatively small subducted geochemical component compared to lavas of other compositions in Ecuador. Andesite, dacite and rhyolites with relatively high incompatible element concentrations (e.g, >30ppm Rb) commonly have isotope ratios (not shown here) that are more crustal (e.g., lower $^{143}Nd/^{144}Nd$) than the main cluster of andesite-dacite data with lower incompatible element concentrations (e.g., Rb<30 ppm; see also Figs. 15-16). Ecuador data are from Table 1. Symbols used here are as in figure 3. Values for MORB are from Sun and McDonough (1989).

Fig. 8 Isotope correlation diagram for Nd and Sr, showing the compositions of lavas from Ecuador compared to data from the Galapagos plume and Carnegie Ridge (White *et al.*, 1993; Harpp & White, 2001), the Andean central and southern volcanic zones (Frey *et al.*, 1984; Hickey *et al.*, 1986; Davidson *et al.*, 1988; Futa & Stern, 1988; Hildreth & Moorbath, 1988; Wörner, 1989; Davidson *et al.*, 1990; Walker *et al.*, 1991), Pacific pelagic sediments (Ben Othman *et al.*, 1989), average upper crust (Zartman & Haines, 1988), Mesozoic oceanic terranes in Colombia and Ecuador (Kerr *et al.*, 1997; Bosch *et al.*, 2002), and upper crust / metamorphic basement in Ecuador (Bosch *et al.*, 2002). Ecuador data are from Table 2. Symbols are as in figure 3.

Fig. 9 Lead isotope correlation diagram for $^{207}Pb/^{204}Pb$ and $^{206}Pb/^{204}Pb$ showing the compositions of lavas from Ecuador compared to data from the Galapagos plume and Carnegie Ridge (White *et al.*, 1993; Harpp & White, 2001), the Andean central and southern volcanic zones (Hickey *et al.*, 1986; Davidson *et al.*, 1988; Hildreth & Moorbath, 1988; Wörner, 1989; Davidson *et al.*, 1990), Pacific pelagic sediments (Ben Othman *et al.*, 1989), average upper crust (Zartman & Haines, 1988), Mesozoic oceanic terranes in Ecuador (Bosch *et al.*, 2002), and upper crust / metamorphic basement in Ecuador (Bosch *et al.*, 2002). Ecuador data are from Table 2. Symbols are as in figure 3.

Fig. 10 Trace element ratios Ba/La, La/Yb and Sr/Y versus SiO_2 comparing lavas from Ecuador to those from the Andean central and southern volcanic zones. Note the similarly high Sr/Y and La/Yb in the andesite compositional range throughout the Andes, but the contrastingly high and variable Ba/La in Ecuador compared to the central and southern Andes. Ecuador data are from Table 1. Symbols are as in figure 3. Published data sources for the central and southern Andes are listed in the captions to figures 6, 8 and 9.

Fig. 11 Trace element concentrations and ratios plotted against distance from trench across Ecuador, showing cross-arc changes in Ba and La concentrations and in La/Yb and Ba/Nb in lavas produced at different positions across the arc. Data plotted here are from Table 1.

Fig. 12 Isotope correlations and mixing/assimilation calculations using Δ7/4Pb and $^{143}Nd/^{144}Nd$. Mixing lines (labeled 1-4) are between estimated Ecuador basalt (3 ppm Pb, 5 ppm Nd, $^{143}Nd/^{144}Nd$=0.512960, εNd=6.3, $^{207}Pb/^{204}Pb$=15.580, $^{206}Pb/^{204}Pb$=19.000) and putative crustal assimilants with isotopic compositions like those of Ecuador metapelites ($^{143}Nd/^{144}Nd$=0.512183, εNd=-8.9, $^{207}Pb/^{204}Pb$=15.700 and $^{206}Pb/^{204}Pb$=18.916). The isotopic composition of the metapelite end-member is from Bosch et al., (2002). Mixing line 1 uses the Pb and Nd concentrations of the average metapelites (Nd=25 ppm, Pb=15 ppm). Subsequent mixing lines use higher Pb concentrations for the assimilant (higher Pb/Nd in the metapelite end-member) to produce the curved mixing lines, which bracket the Ecuador lavas (Pb/Nd=1.2 and 4.0). These calculations suggest that most of the Ecuador lavas that appear to have assimilated local crustal rocks (i.e., those with Δ7/4Pb>7.0) can be explained by the addition of no more than approximately 5-10% of country rock that is geochemically similar to the Ecuador metapelites. Selection of the isotopic composition for the basalt end-member (offset from Carnegie Ridge compositions toward lower $^{143}Nd/^{144}Nd$=0.512910, and higher $^{207}Pb/^{204}Pb$=15.605) at the margin of the field for Galapagos basalt is consistent with presumed additions of seawater and sediment to the subducting oceanic crust beneath Ecuador. Concentrations for Nd and Pb in the basalt end-member were estimated by extrapolating andesite compositions for these elements back to approximately 52% SiO_2. Values for Δ7/4Pb were calculated according as in Hart (1984).

Fig. 13 Isotope ratios plotted against distance from trench across Ecuador, showing cross-arc changes in $^{87}Sr/^{86}Sr$, $^{143}Nd/^{144}Nd$ and Δ7/4 Pb in lavas produced at different positions across the arc. Data plotted here are from Table 2. Symbols used here are as in figure 3.

Fig. 14 Neodymium isotope ratios plotted against trace element concentrations, showing decreasing average $^{143}Nd/^{144}Nd$ in andesite, dacite and rhyolite samples with increasing concentrations of Nb, Zr, Rb and Ba. This inverse isotope-trace element relationship is less clear for Sr and appears to be nearly absent for Y. Data plotted here are from Tables 1 and 2. Symbols used here are as in figure 3.

Fig. 15 Neodymium (Nd) and Pb isotopes plotted against La/Yb, Ba/La and Sr/Y for Ecuador lavas. Figure 15A and B show decrease in average $^{143}Nd/^{144}Nd$ for andesites, dacites and rhyolites with La/Yb>12 and Δ7/4Pb>7.0. Decreasing average $^{143}Nd/^{144}Nd$ and Δ7/4Pb at higher La/Yb, which is also evident in cross-arc changes in these geochemical parameters (Figs. 11, 13), is interpreted to be a product of crustal assimilation. Figure 15C and D similarly show decreasing $^{143}Nd/^{144}Nd$ and Δ7/4Pb with decreasing Ba/Nb, a trend that is also interpreted to be a product of crustal assimilation. Large white arrows on Ba/Nb plots provide an interpretation of source components in the mantle wedge (low Δ7/4Pb, Ba/Nb, high $^{143}Nd/^{144}Nd$), fluids and/or melts from the subducting oceanic crust (low Δ7/4Pb, high Ba/Nb, $^{143}Nd/^{144}Nd$) and continental crust assimilant (high Δ7/4Pb, low Ba/Nb, $^{143}Nd/^{144}Nd$). Figures 15E and F show that there is no clear relationship between Sr/Y and isotope composition for Ecuador lavas. Data plotted here are form Tables 1 and 2. Symbols used are as in figure 3.

Fig. 16 Isotopic compositions for Sr, Nd, and Pb in Ecuador lavas (large symbols) and other areas with the Andes (small symbols) plotted as a function of SiO_2. Figures 16A, B, C demonstrate that, except for a broad increase in Δ7/4 Pb with increasing SiO_2, there is relatively little systematic relationship between isotopic compositions and silica content in volcanic rocks from Ecuador. Figure 16D illustrates the uniformly more primitive isotopic compositions of the Ecuador lavas ($^{87}Sr/^{86}Sr<0.7045$) compared to lavas of the central and southern Andes, which are variable and relatively radiogenic ($^{87}Sr/^{86}Sr>0.7050$). Ecuador data are form Tables 1 and 2. Sources for central and southern Andes data are cited in the caption to figure 8.

Fig. 17

REFERENCES

Arculus, R. J., Lapierre, H., and Jaillard, E. (1999). Geochemical window into subduction and accretion processes: Raspas metamorphic complex, Ecuador. *Geology* **27**, 547-550.

Barazangi, M., and Isacks, B. (1976). Spatial distribution of earthquakes and subduction of the Nazca plate beneath South America. *Geology* **4**, 686-692.

Barragan, R., Geist, D., Hall, M., Larsen, P., and Kurz, M. (1998). Subduction controls on the compositions of lavas from the Ecuadorian Andes. *Earth and Planetary Science Letters* **154**, 153-166.

Beate, B., Monzier, M., Spikings, R., Cotten, J., Silva, J., Bourdon, E., and Eissen, J. P. (2001). Mio-Pliocene adakite generation related to flat subduction in southern Ecuador: the Quimsacocha volcanic center. *Earth and Planetary Science Letters* **192**, 561-570.

Bourdon, E., Eissen, J. P., Gutscher, M. A., Monzier, M., Hall, M. L., and Cotten, J. (2003). Magmatic response to early aseismic ridge subduction: The Ecuadorian margin case (South America). *Earth and Planetary Science Letters* **205**, 123-138.

Bourdon, E., Eissen, J. P., Monzier, M., Robin, C., Martin, H., Cotten, J., and Hall, M. L. (2002). Adakite-like Lavas from Antisana Volcano (Ecuador): Evidence for Slab Melt Metasomatism Beneath Andean Northern Volcanic Zone. *Journal of Petrology* **43**, 199-127.

Castillo, P. R., Janney, P. E., and Solidum, R. U. (1999). Petrology and geochemistry of Camiguin Island, southern Philippines: insights to the source of adakites and other lavas in a complex arc setting. *Contributions to Mineralogy and Petrology* **134**, 33-51.

Class, C., Miller, D. M., Goldstein, S. L., and Langmuir, C. H. (2000). Distinguishing melt and fluid subduction components in Umnak Volcanics, Aleutian Arc. *Geochemistry, Geophysics, Geosystems* 1999GC000010.

Conrad, W. K., and Kay, R. W. (1984). Ultramafic and mafic inclusions from Adak Island: crystallization history, and implications for the nature of primary magmas and crustal evolution in the Aleutian arc. *Journal of Petrology* **25**, 88-125.

Davidson, J., Tepley, F., Palacz, Z., and Meffan-Main, S. (2000). Magma recharge, contamination and residence times revealed by in situ laser ablation isotopic analysis of feldspar in volcanic rocks. *Earth and Planetary Science Letters* **184**, 427-442.

Davidson, J. P., McMillan, N. J., Moorbath, S., Wörner, G., Harmon, R. S., and Lopez-Escobar, L. (1990). The Nevados de Payachata volcanic region (18°S/69°W, N. Chile); II, Evidence for widespread crustal involvement in Andean magmatism. *Contributions to Mineralogy and Petrology* **105**, 412-432.

Defant, M. J., and Drummond, M. S. (1990). Derivation of some modern arc magmas by melting of young subducted lithosphere. *Nature* **347**, 662-665.

DePaolo, D. J. (1981). Trace element and isotopic effects of combined wallrock assimilation and fractional crystallization. *Earth and Planetary Science Letters* **53**, 189-202.

Dickinson, W. R. (1975). Potash-depth (K-h) relations in continental margin and intra-oceanic magmatic arcs. *Geology* **3**, 53-56.

Drummond, M. S., and Defant, M. J. (1990). A model for trondhjemite-tonalite-dacite genesis and crustal growth via slab melting: Archean to modern comparisons. *Journal of Geophysical Research* **95**, 21503-21521.

Elliott, T., Plank, T., Zindler, A., White, W., and Bourdon, B. (1997). Element transport from slab to volcanic front at the Mariana arc. *Journal of Geophysical Research* **102**, 14,991-15,019.

Feininger, T. (1987). Allochthonous terranes in the Andes of Ecuador and northwesern Peru. *Canadian Journal of Earth Science* **24**, 266-278.

Feininger, T., and Seguin, M. K. (1983). Bouguer gravity anomaly field and inferred crustal structure of continental Ecuador. *Geology* **11**, 40-44.

Garrison, J. M., and Davidson, J. P. (2003). Dubious case fo slab melting in the Northern volcanic zone of the Andes. *Geology* **31**, 565-568.

Gill, J. (1981). *Orogenic Andesites and Plate Tectonics*. New York: Springer-Verlag, 390 pp.

Gutscher, M. A., Malavieille, J., Lallemand, S., and Collot, J. Y. (1999a). Tectonic segmentation of the North Andean margin: impact of the Carnegie Ridge collision. *Earth and Planetary Science Letters* **168**, 255-270.

Gutscher, M. A., Maury, R. C., Eissen, J. P., and Bourdon, E. (2000a). Can slab melt be caused by flat slab? *Geology* **28**, 535-538.

Gutscher, M. A., Olivet, J. L., Aslanian, D., Eissen, J. P., and Maury, R. C. (1999b). The "lost Inca Plateau": Cause of flat subduction beneath Peru? *Earth and Planetary Science Letters* **171**, 335-341.

Gutscher, M. A., Spakman, W., Bijwaard, H., and Engdahl, E. R. (2000b). Geodynamics of flat subduction: seismicity and tomographic constraints from the Andean margin. *Tectonics* **19**, 814-832.

Hall, M. L., and Calle, J. (1982). Geochronological control for the main tectonic-magmatic events of Ecuador. *Earth Science Reviews* **18**, 215-239.

Harmon, R. S., Barreiro, B., Moorbath, S., Hoefs, J., Francis, P. W., Thorpe, R. S., Deruelle, B., McHugh, J., and Viglino, J. A. (1984). Regional O-, Sr-, and Pb-isotope relationships in the late Cenozoic calc-alkaline lavas of the Andean Cordillera. *Journal of the Geological Society of London* **141**, 803-822.

Hart, S. R. (1984). A large-scale isotope anomaly in the Southern Hemisphere mantle. *Nature* **309**, 753-757.

Hildreth, W., and Moorbath, S. (1988). Crustal contribtutions to arc magmatism in the Andes of central Chile. *Contributions to Mineralogy and Petrology* **98**, 455-489.

Holbrook, S. W., D.Lizarralde, S.McGeary, Bangs, N., and Diebold, J. (1999). Structure and composition of the Aleutian island arc and implications for continental crustal growth. *Geology* **27**, 31-34.

Hörmann, P. K., and Pichler, H. (1982). Geochemistry, petrology and origin of the Cenozoic volcanic rocks of the Northern Andes in Ecuador. *Journal of Volcanology and Geothermal Research* **12**, 259-282.

Hughes, R. A., and Pilatasig, L. F. (2002). Cretaceous and Tertiary terrane accretion in the Cordillera Occidental of the Andes of Ecuador. *Tectonophysics* **345**,

James, D. E. (1982). A combined O, Sr, Nd, and Pb isotopic and trace element study of crustal contamination in central Andean lavas, I. Local geochemical variations. *Earth and Planetary Science Letters* **57**, 47-62.

James, D. E., and Murcia, L. A. (1984). Crustal contamination in northern Andean volcanics. *Journal of the Geological Society of London* **141**, 823-830.

Johnson, D. M., Hooper, P. R., and Conrey, R. M. (1999). XRF analysis of rocks and minerals for major and trace elements on a single low-dilution Li-tetraborate fused bead. *Advances in X-ray Analysis* **41**, 117-132.

Kay, R. W. (1978). Aleutian magnesian andesites: melts from subducted Pacific ocean crust. *Journal of Volcanology and Geothermal Research* **4**, 117-132.

- (1980). Volcanic arc magma genesis: implications for element recycling in the crust-upper mantle system. *Journal of Geology* **88**, 497-522.

Kay, R. W., and Kay, S. M. (1991). Creation and destruction of lower continental crust. *Geologische Rundschau* **80**, 259-278.

Kay, R. W., Sun, S. S., and Lee-Hu, C. N. (1978). Pb and Sr isotopes in volcanic rocks from the Aleutian Islands and Pribilof Islands, Alaska. *Geochimica et Cosmochimica Acta* **42**, 263-273.

Kay, S. M., Maksaev, V., Moscoso, R., Mpodozis, C., and Nasi, C. (1987). Probing the evolving Andean lithosphere: mid-late Tertiary magmatism in Chile (29 -30 30'S) over the modern zone of subhorizontal subduction. *Journal of Geophysical Research* **92**, 6173-6189.

Kay, S. M., Maksaev, V., Moscoso, R., Mpodozis, C., Nasi, C., and Gordillo, C. E. (1988). Tertairy Andean magmatism in Chile and Argentina between 28 S and 33 S: Correlation of magmatic chemistry with a changing Benioff zone. *Journal of South American Earth Sciences* **1**, 21-38.

Kay, S. M., Ramos, V. A., and Marquez, Y. M. (1993). Evidence in Cerro Pampa volcanic rocks for slab-melting prior to ridge-trench collision in southern South America. *Journal of Geology* **101**, 703-714.

Kelemen, P. B. (1995). Genesis of high Mg# andesites and the continental crust. *Contributions to Mineralogy and Petrology* **120**, 1-19.

Kelemen, P. B., Yogodzinski, G. M., and Scholl, D. W. (2003). Along-strike variation in lavas of the Aleutian Island Arc: Implications for the genesis of high Mg# andesite and the continental crust. In: Eiler, J. (ed.) Inside the Subduction Factory, Geophysical Monograph 138. Washington D.C.: American Geophysical Union, 223-276.

Kellogg, J. N., and Vega, V. (1995). Tectonic development of Panama, Costa Rica, and the Colombian Andes: Constraints from global positioning system geodetic studies and gravity. In: Mann, P. (ed.) Geologic and Tectonic Development of the Caribbean Plate Boundary in Southern Central America, Geological Society of America Special Paper 295. Boulder: Geological Society of America, 75-89.

Kepezhinskas, P., McDermott, F., Defant, M. J., Hochstaedter, A., Drummond, M. S., Hawkesworth, C. J., Koloskov, A., Maury, R. C., and Bellon, H. (1997). Trace element and Sr-Nd-Pb isotopic constraints on a three-component model of Kamchatka arc petrogenesis. *Geochimica et Cosmochimica Acta* **61**, 577-600.

Kilian, R., Hegner, E., Fortier, S., and Satir, M. (1994). The genesis of Quaternary volcanic rocks in contrasting lithospheric settings of Ecuador. *7th Chilean Geologic Congress Abstracts* **2**, 1378-1382.

- (1995). Magma evolution within the accretionary mafic basement of Quaternary Chimborazo and associated volcanos (Western Ecuador). *Revista Geological de Chile* **22**, 203-208.

Kilian, R., and Pichler, H. (1989). The Northandean volcanic zone. *Zentralblatt für Geologie und Paläontologie, Teil I* **5/6**, 1075-1085.

Lichte, F. E., Meier, A. L., and Crock, J. G. (1987). Determination of rare-earth elements in geological materials by inductively coupled plasma mass spectrometry. *Analytical Chemistry* **59**, 1150-1157.

Litherland, M., Aspden, J. A., and Jemielita, R. A. (1994). *The Metamorphic Belts of Ecuador*. British Geological Survey, 147 pp.

Monzier, M., Robin, C., Samaniego, P., Hall, M. L., Cotten, J., Mothes, P., and Arnaud, N. (1999). Sangay Volcano, Ecuador: structural development, present activity and petrology. *Journal of Volcanology and Geothermal Research* **90**, 49-79.

Morris, J. D., Leeman, W. P., and Tera, F. (1990). The subducted component in island arc lavas: constraints from Be isotopes and B-Be systematics. *Nature* **344**, 31-35.

Noble, S. R., Aspden, J. A., and Jemielita, R. A. (1997). Northern Andean crustal evolution: New U-Pb geochronological constraints from Ecuador. *Geological Society of America Bulletin* **109**, 789-798.

Petford, N., and Atherton, M. (1996). Na-rich partial melts from newly underplated basaltic crust: the Cordillera Blanca Batholith, Peru. *Journal of Petrology* **37**, 1491-1521.

Pichler, J., Hörmann, P. K., and Braun, A. F. (1976). First petrologic data on lavas of the Volcano El Reventador (Eastern Ecuador). *Münstersche Forschungen zur Geologie und Palaontologie* **38**, 129-141.

Plank, T., and Langmuir, C. H. (1993). Tracing trace elements from sediment input to volcanic output at subduction zones. *Nature* **362**, 739-742.

Rapp, R. P., Shimizu, N., Norman, M. D., and Applegate, G. S. (1999). Reaction between slab-derived melts and peridotite in the mantle wedge: Experimental constraints at 3.8 GPa. *Chemical Geology* **160**, 335-356.

Rogers, G., Saunders, A. D., Terrell, D. J., Verma, S. P., and Marriner, G. F. (1985). Geochemistry of Holocene volcanic rocks associated with ridge subduction in Baja, California, Mexico. *Nature* **315**, 389-392.

Salvador, M. E., and Kellogg, J. N. (1991). Gravity field, crustal structure and effective elastic thickness of the North Andes. *Eos Spring Supplement* **72**, 91.

Samaniego, P., Martin, H., Robin, C., and Monzier, M. (2002). Transition from calc-alkalic to adakitic magmatism at Cayambe volcano, Ecuador: Insights into slab melts and mantle wedge interactions. *Geology* **30**, 967-970.

Saunders, A. D., Rogers, G., Marriner, G. F., Terrell, D. J., and Verma, S. P. (1987). Geochemistry of Cenozoic volcanic rocks, Baja California, Mexico: implications for the petrogenesis of post-subduction magmas. *Journal of Volcanology and Geothermal Research* **32**, 223-245.

Singer, B. S., and Myers, J. D. (1990). Intra-arc extension and magmatic evolution in the central Aleutian arc, Alaska. *Geology* **18**, 1050-1053.

Stern, C. R., and Killian, R. (1996). Role of the subducted slab, mantle wedge and continental crust in the generation of adakites from the Andean Austral Volcanic Zone. *Contributions to Mineralogy and Petrology* **123**, 263-281.

Stern, C. R., and Wyllie, P. J. (1978). Phase compositions through crystallization intervals in basalt - andesite - H2O at 30 kbar with implications for subduction zone magmas. *American Mineralogist* **63**, 641-663.

van der Hilst, R., and Mann, P. (1994). Tectonic implications of tomographic images of subducted lithosphere beneath northwesern South America. *Geology* **22**, 451-454.

Vanek, J., Vankova, V., and Hanus, V. (1994). Geochemical zonation of volcanic rocks and deep structure of Ecuador and southern Columbia. *Journal of South American Earth Sciences* **7**, 57-67.

von Huene, R., and Scholl, D. W. (1991). Observations at convergent margins concerning sediment subduction, subduction erosion, and the growth of continental crust. *Reviews of Geophysics* **29**, 279-316.

Woodhead, J. D. (1988). The origin of geochemical variations in Mariana lavas: a general model for petrogenesis in intra-oceanic island arcs? *Journal of Petrology* **29**, 805-830.

Yogodzinski, G. M., Kay, R. W., Volynets, O. N., Koloskov, A. V., and Kay, S. M. (1995). Magnesian andesite in the western Aleutian Komandorsky region: Implications for slab melting and processes in the mantle wedge. *Geological Society of America Bulletin* **107**, 505-519.

Yogodzinski, G. M., and Kelemen, P. B. (1998). Slab melting in the Aleutians: implications of an ion probe study of clinopyroxene in primitive adakite and basalt. *Earth and Planetary Science Letters* **158**, 53-65.

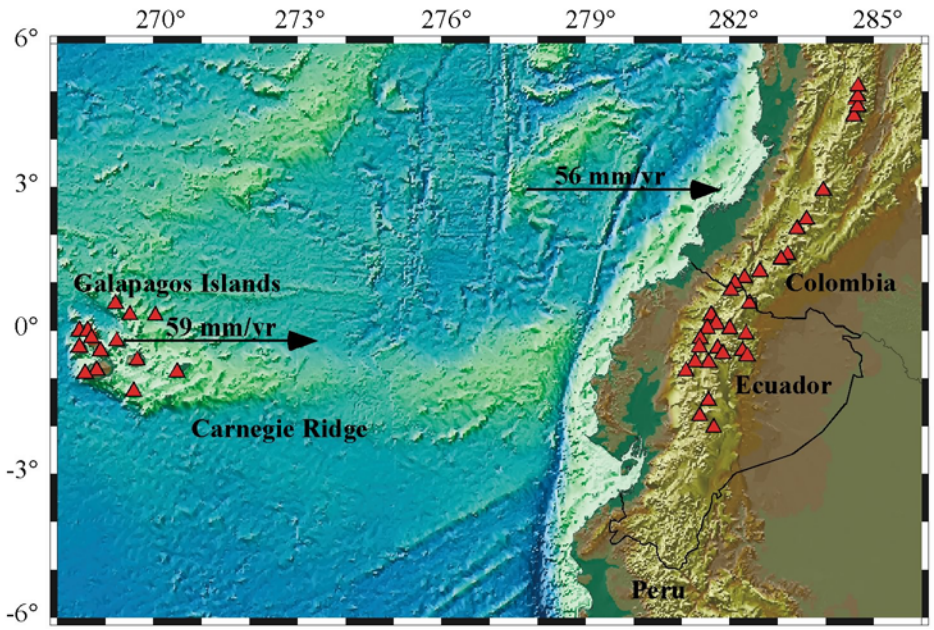
270°
273°
276°
279°
282°
285°
6°
3°
0°
-3°
-6°
56 mm/yr
59 mm/yr
Galapagos Islands
Carnegie Ridge
Colombia
Ecuador
Peru

FIGURE 1

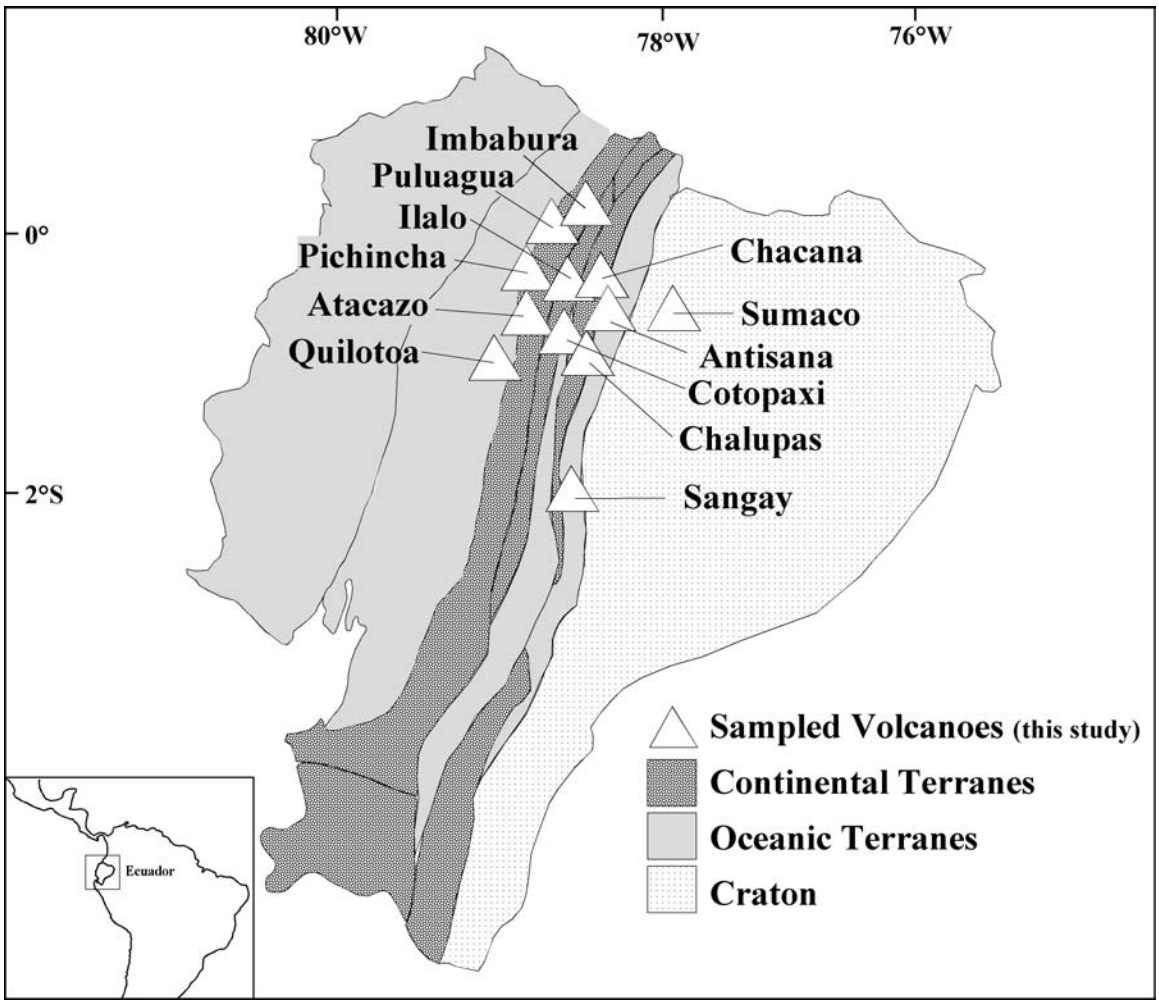
80°W
78°W
76°W
0°
2°S
Imbabura
Puluagua
Ilalo
Pichincha
Atacazo
Quilotoa
Chacana
Sumaco
Antisana
Cotopaxi
Chalupas
Sangay
Ecuador
Sampled Volcanoes (this study)
Continental Terranes
Oceanic Terranes
Craton

FIGURE 2

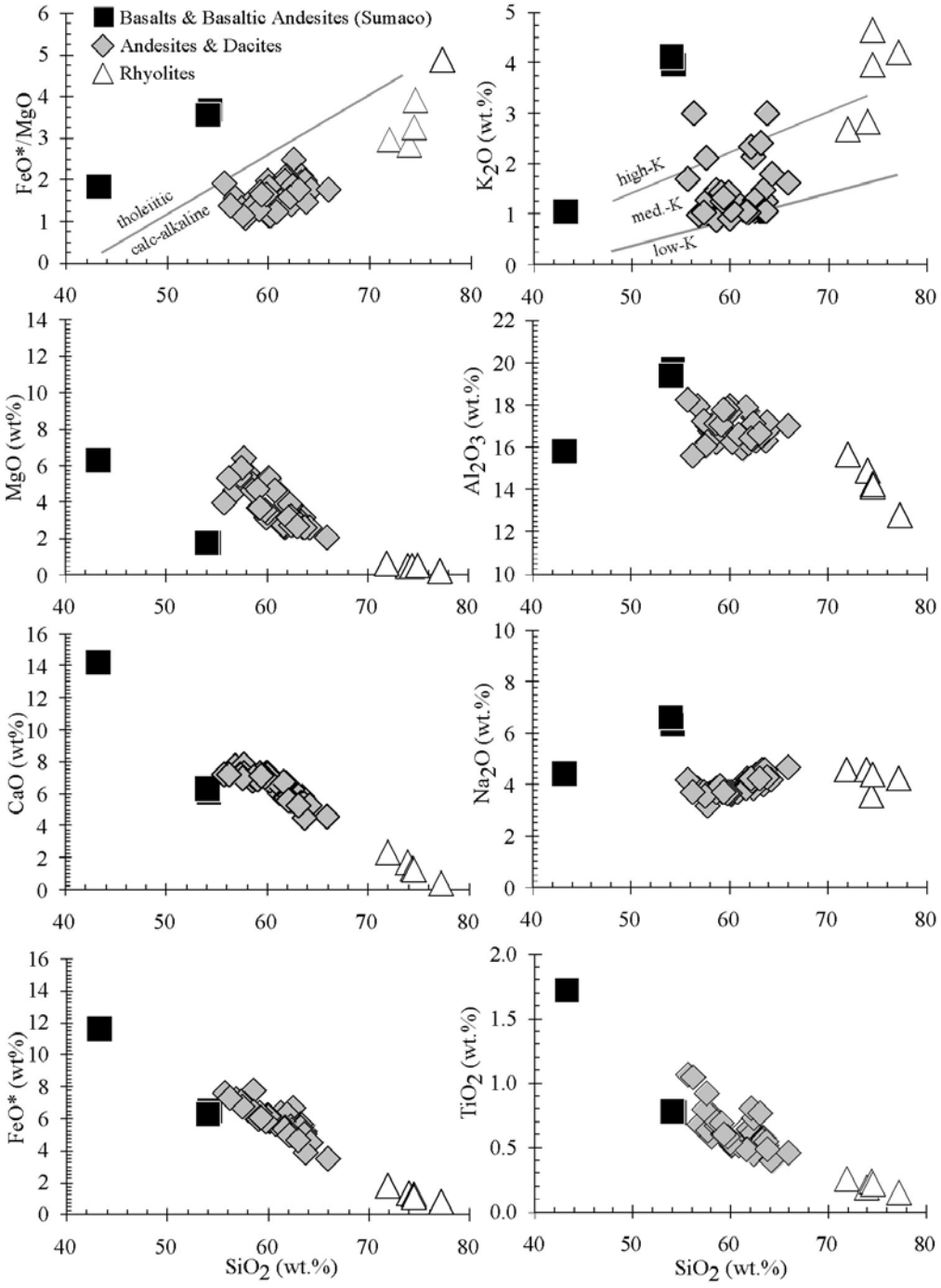
Basalts & Basaltic Andesites (Sumaco)
Andesites & Dacites
Rhyolites
FeO*/MgO
tholeiitic
calc-alkaline
K2O (wt.%)
high-K
med.-K
low-K
MgO (wt%)
Al2O3 (wt.%)
CaO (wt%)
Na2O (wt.%)
FeO* (wt%)
TiO2 (wt.%)
SiO2 (wt.%)
SiO2 (wt.%)

FIGURE 3

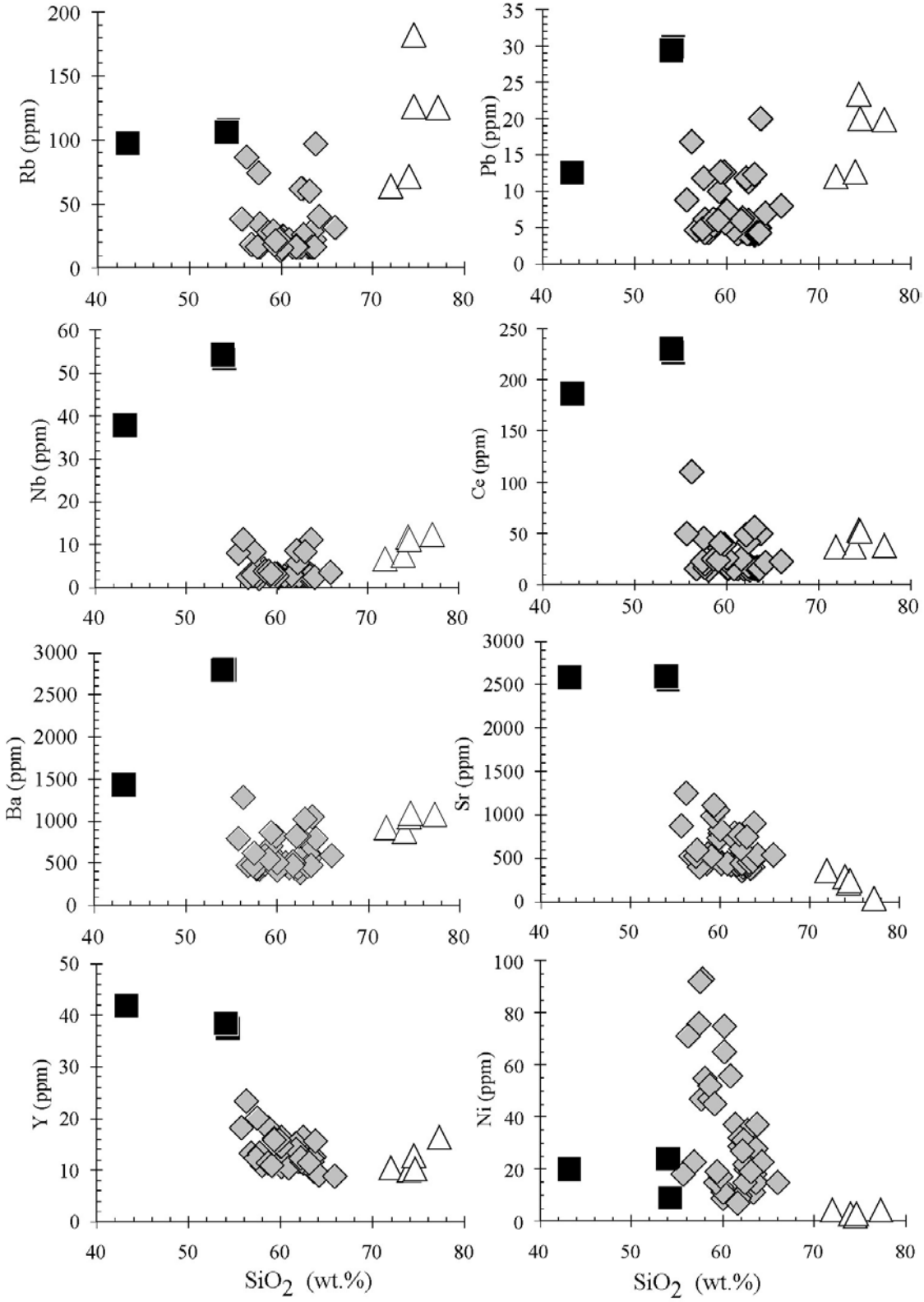
Rb (ppm)
Pb (ppm)
Nb (ppm)
Ce (ppm)
Ba (ppm)
Sr (ppm)
Y (ppm)
Ni (ppm)
SiO2 (wt.%)
SiO2 (wt.%)

FIGURE 4

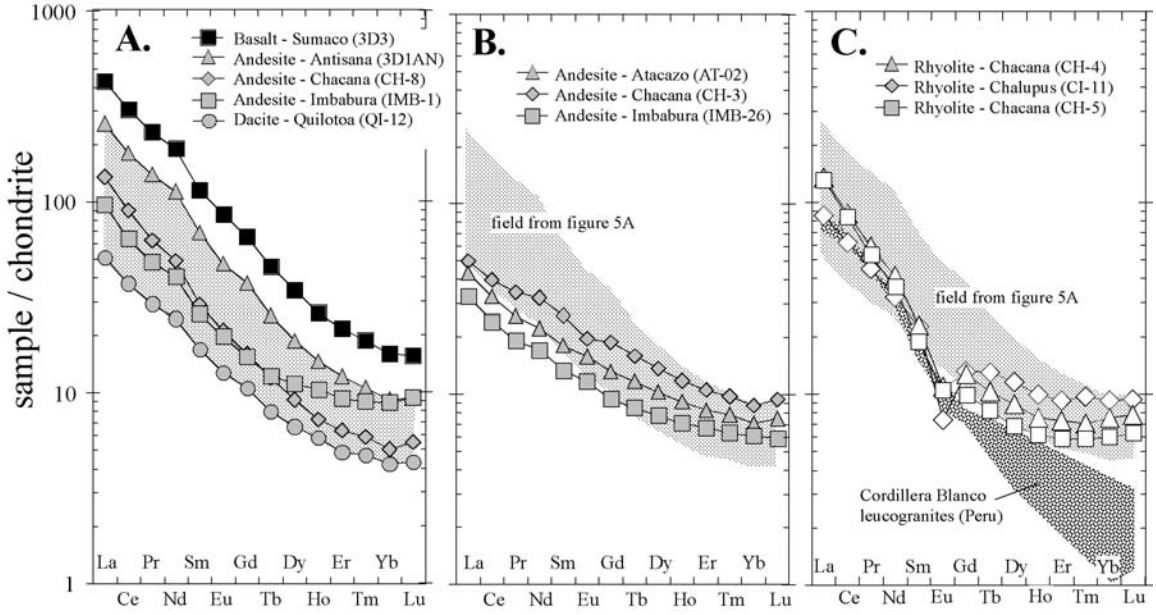
A.
Basalt - Sumaco (3D3)
Andesite - Antisana (3D1AN)
Andesite - Chacana (CH-8)
Andesite - Imbabura (IMB-1)
Dacite - Quilotoa (QI-12)
B.
Andesite - Atacazo (AT-02)
Andesite - Chacana (CH-3)
Andesite - Imbabura (IMB-26)
field from figure 5A
C.
Rhyolite - Chacana (CH-4)
Rhyolite - Chalupus (CI-11)
Rhyolite - Chacana (CH-5)
field from figure 5A
Cordillera Blanco
leucogranites (Peru)
sample / chondrite
1000
100
10
1
La Ce Pr Nd Sm Eu Gd Tb Dy Ho Er Tm Yb Lu

FIGURE 5

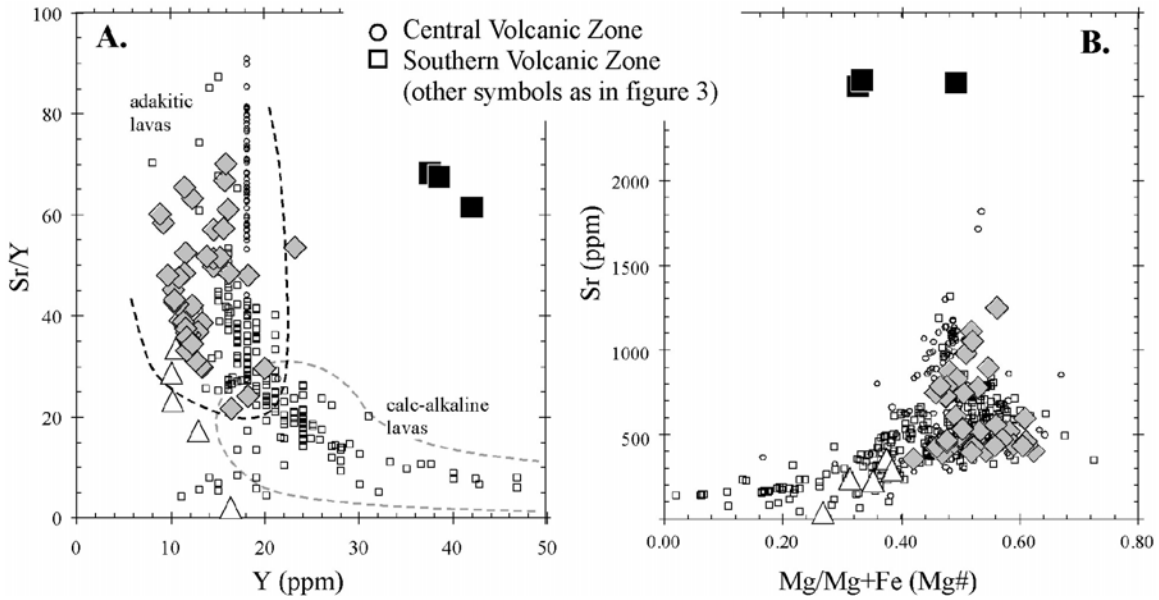
A.
B.
Central Volcanic Zone
Southern Volcanic Zone
(other symbols as in figure 3)
adakitic
lavas
calc-alkaline
lavas
Sr/Y
Y (ppm)
Sr (ppm)
Mg/Mg+Fe (Mg#)
0
20
40
60
80
100
10
30
50
500
1000
1500
2000
0.00
0.20
0.40
0.60
0.80

FIGURE 6

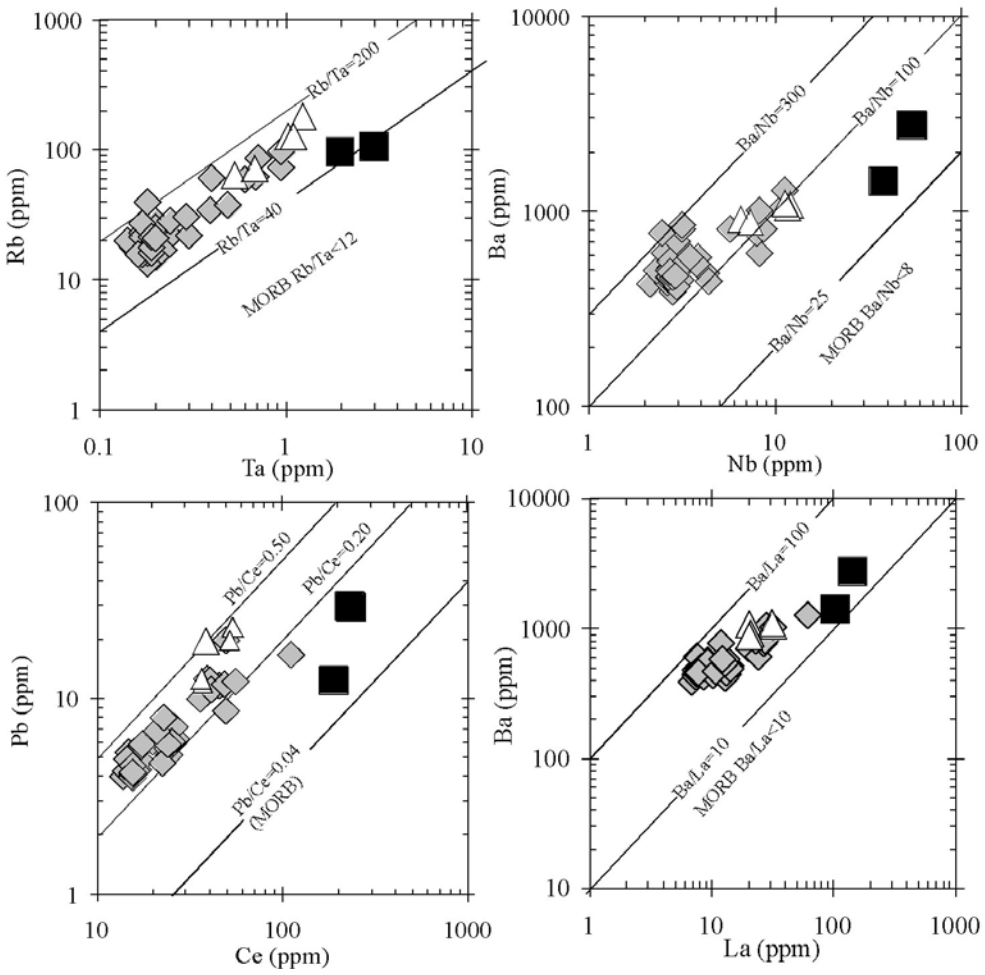
Rb (ppm)
Ta (ppm)
Rb/Ta=200
Rb/Ta=40
MORB Rb/Ta<12
Ba (ppm)
Nb (ppm)
Ba/Nb=300
Ba/Nb=100
Ba/Nb=25
MORB Ba/Nb<8
Pb (ppm)
Ce (ppm)
Pb/Ce=0.50
Pb/Ce=0.20
Pb/Ce=0.04
(MORB)
Ba (ppm)
La (ppm)
Ba/La=100
Ba/La=10
MORB Ba/La<10

FIGURE 7

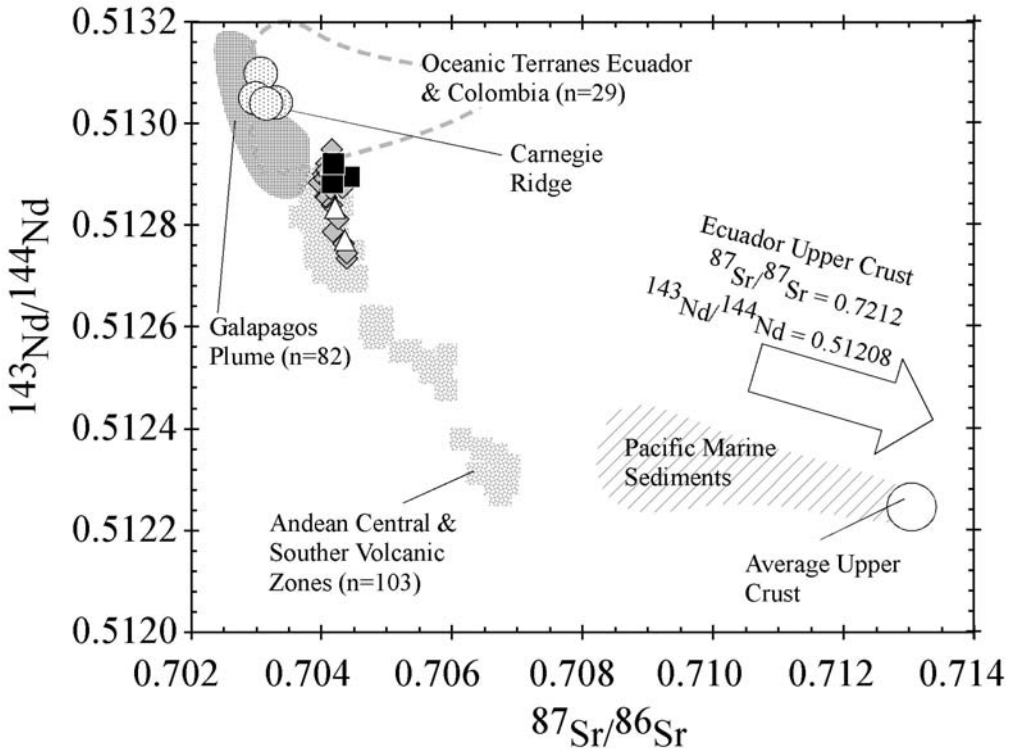
0.5132
0.5130
0.5128
0.5126
0.5124
0.5122
0.5120
0.702
0.704
0.706
0.708
0.710
0.712
0.714
143Nd/144Nd
87Sr/86Sr
Oceanic Terranes Ecuador & Colombia (n=29)
Carnegie Ridge
Galapagos Plume (n=82)
Ecuador Upper Crust
87Sr/87Sr = 0.7212
143Nd/144Nd = 0.51208
Pacific Marine Sediments
Andean Central & Souther Volcanic Zones (n=103)
Average Upper Crust

FIGURE 8

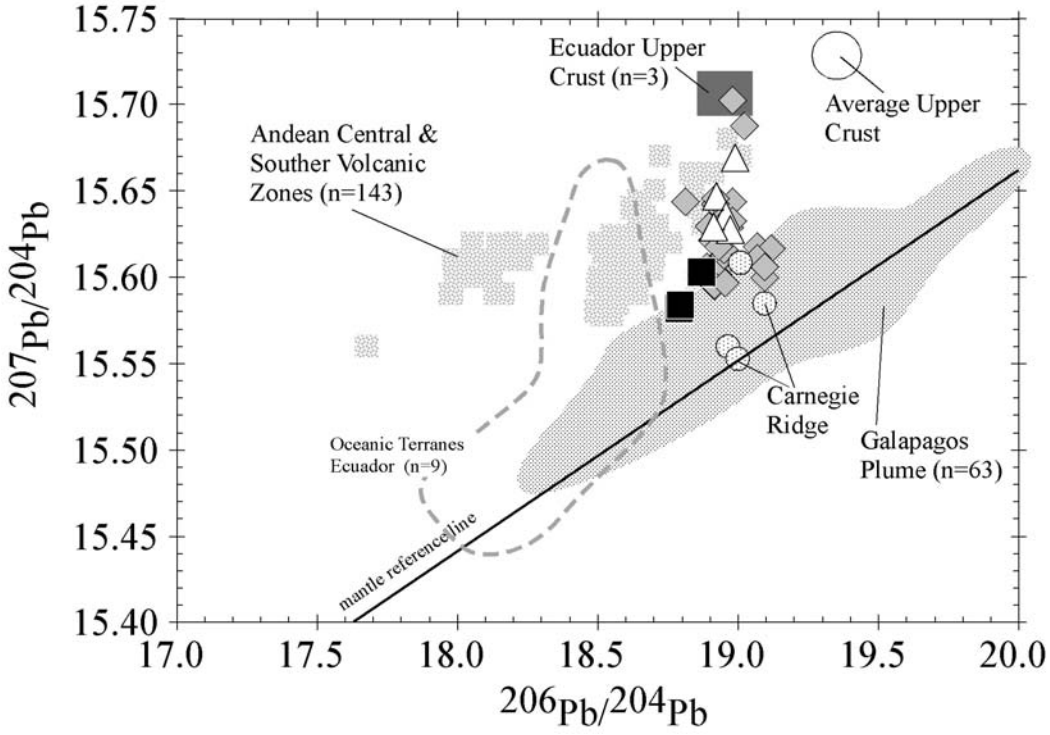
15.75
15.70
15.65
15.60
15.55
15.50
15.45
15.40
17.0
17.5
18.0
18.5
19.0
19.5
20.0
207Pb/204Pb
206Pb/204Pb
Ecuador Upper Crust (n=3)
Average Upper Crust
Andean Central & Souther Volcanic Zones (n=143)
Carnegie Ridge
Galapagos Plume (n=63)
Oceanic Terranes Ecuador (n=9)
mantle reference line

FIGURE 9

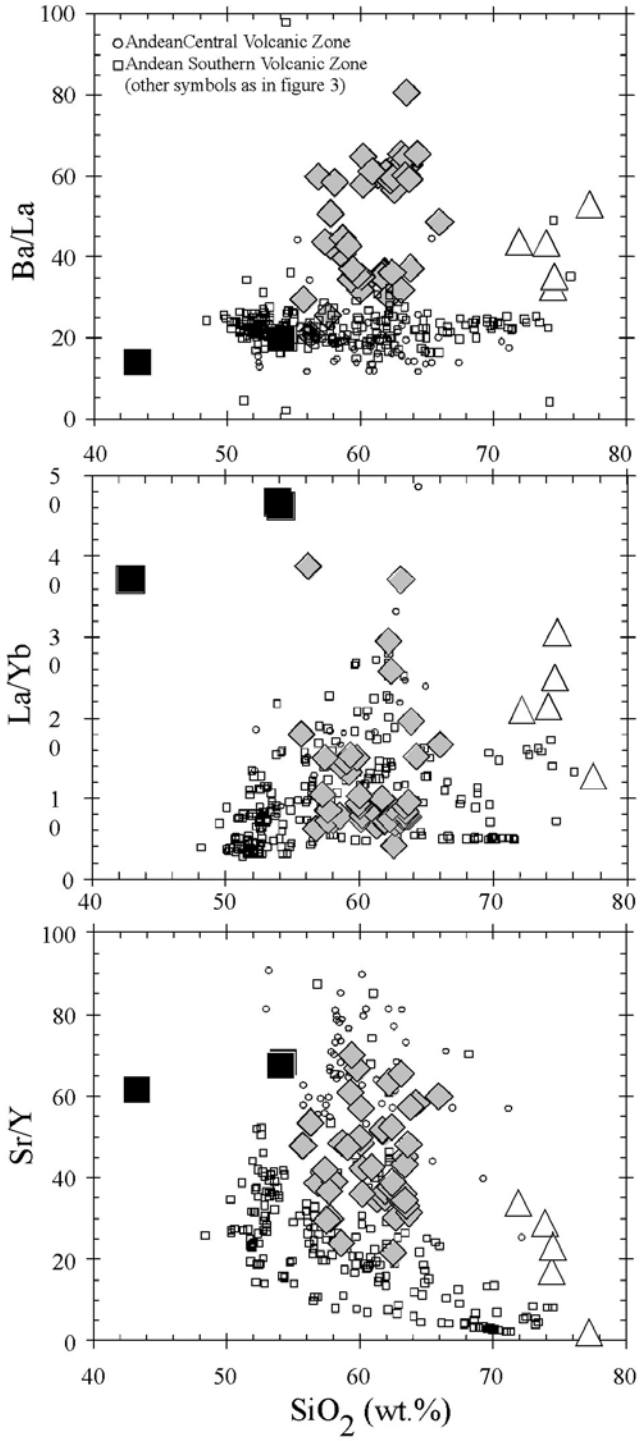
AndeanCentral Volcanic Zone
Andean Southern Volcanic Zone
(other symbols as in figure 3)
Ba/La
La/Yb
Sr/Y
SiO2 (wt.%)

FIGURE 10

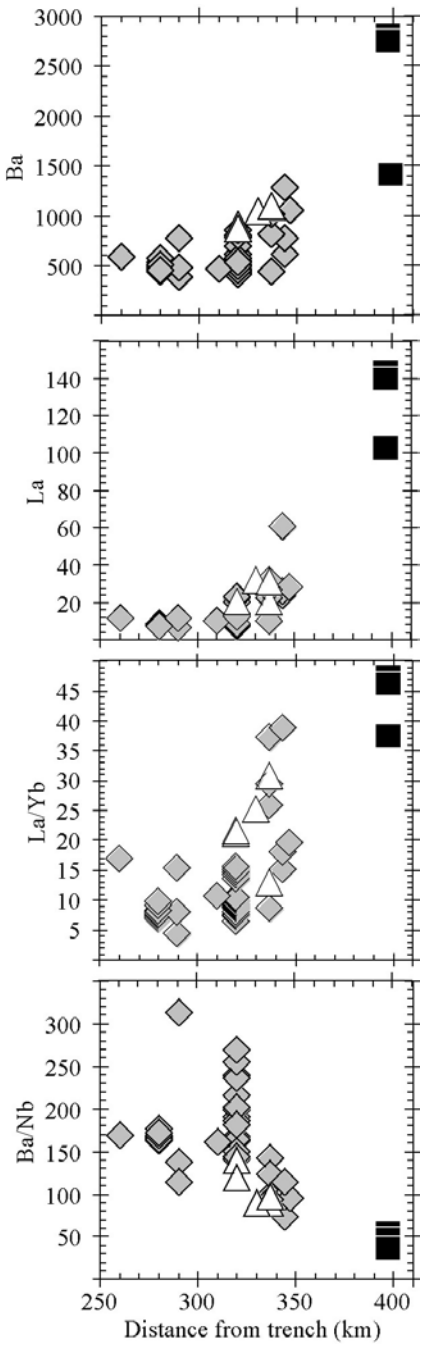

FIGURE 11

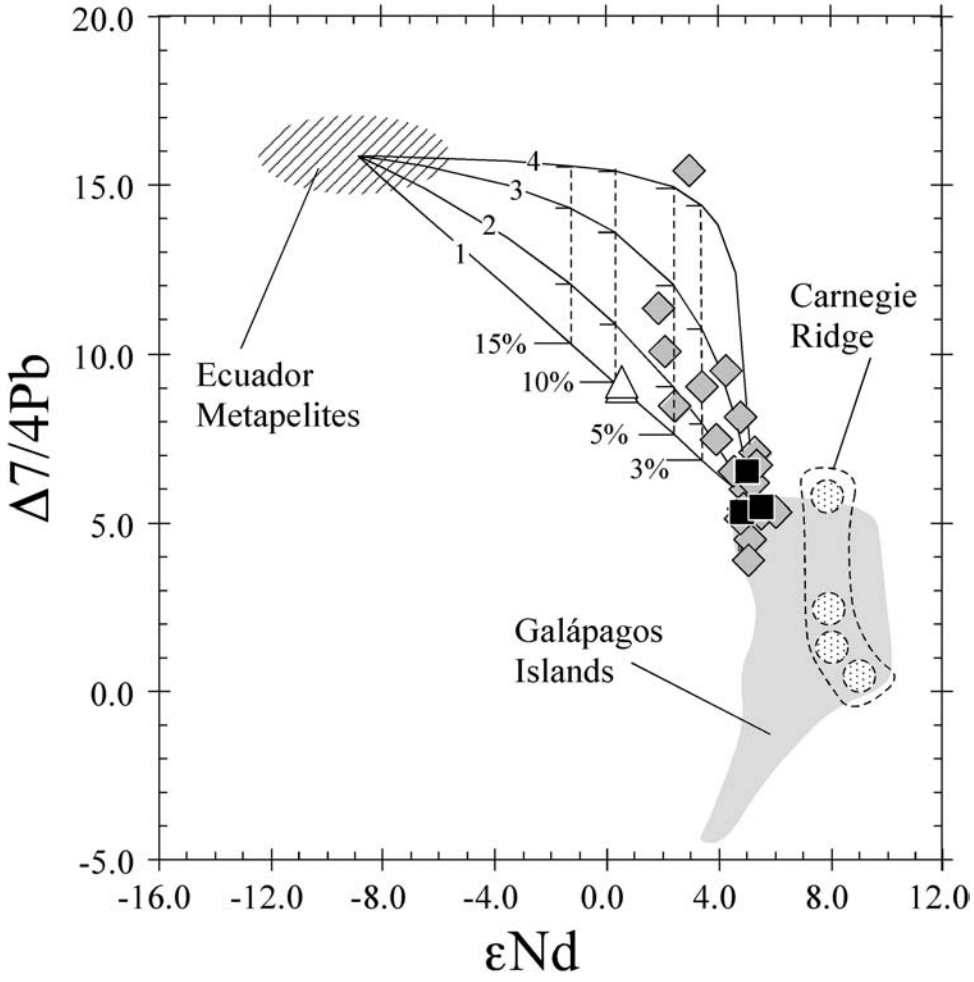
20.0
15.0
10.0
5.0
0.0
-5.0
-16.0
-12.0
-8.0
-4.0
0.0
4.0
8.0
12.0
Δ7/4Pb
εNd
4
3
2
1
15%
10%
5%
3%
Ecuador
Metapelites
Carnegie
Ridge
Galápagos
Islands

FIGURE 12

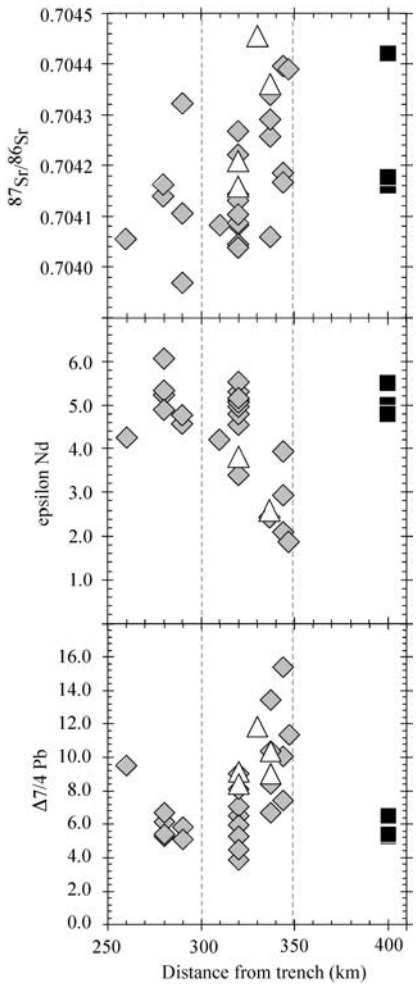
0.7045
0.7044
0.7043
0.7042
0.7041
0.7040
87Sr/86Sr
6.0
5.0
4.0
3.0
2.0
1.0
epsilon Nd
16.0
14.0
12.0
10.0
8.0
6.0
4.0
2.0
0.0
Δ7/4 Pb
250
300
350
400
Distance from trench (km)

FIGURE 13

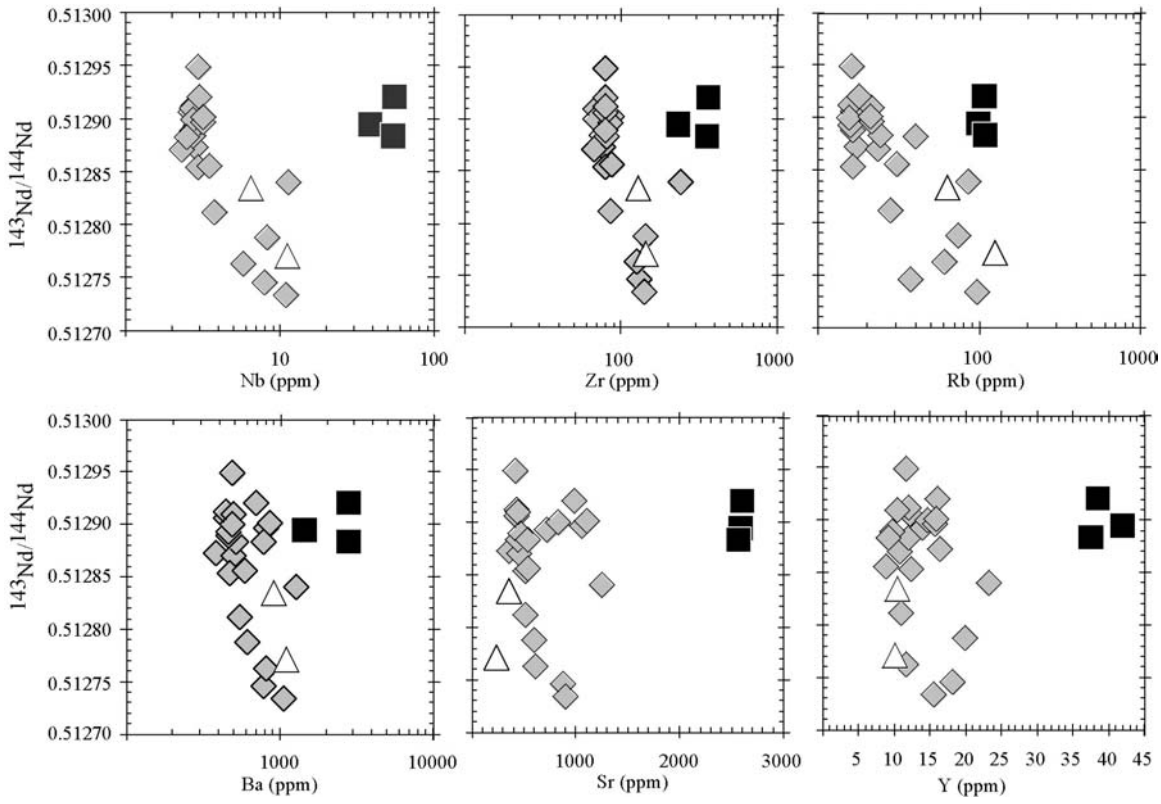
0.51300
0.51295
0.51290
0.51285
0.51280
0.51275
0.51270
143Nd/144Nd
10
100
Nb (ppm)
100
1000
Zr (ppm)
100
1000
Rb (ppm)
1000
10000
Ba (ppm)
1000
2000
3000
Sr (ppm)
5 10 15 20 25 30 35 40 45
Y (ppm)

FIGURE 14

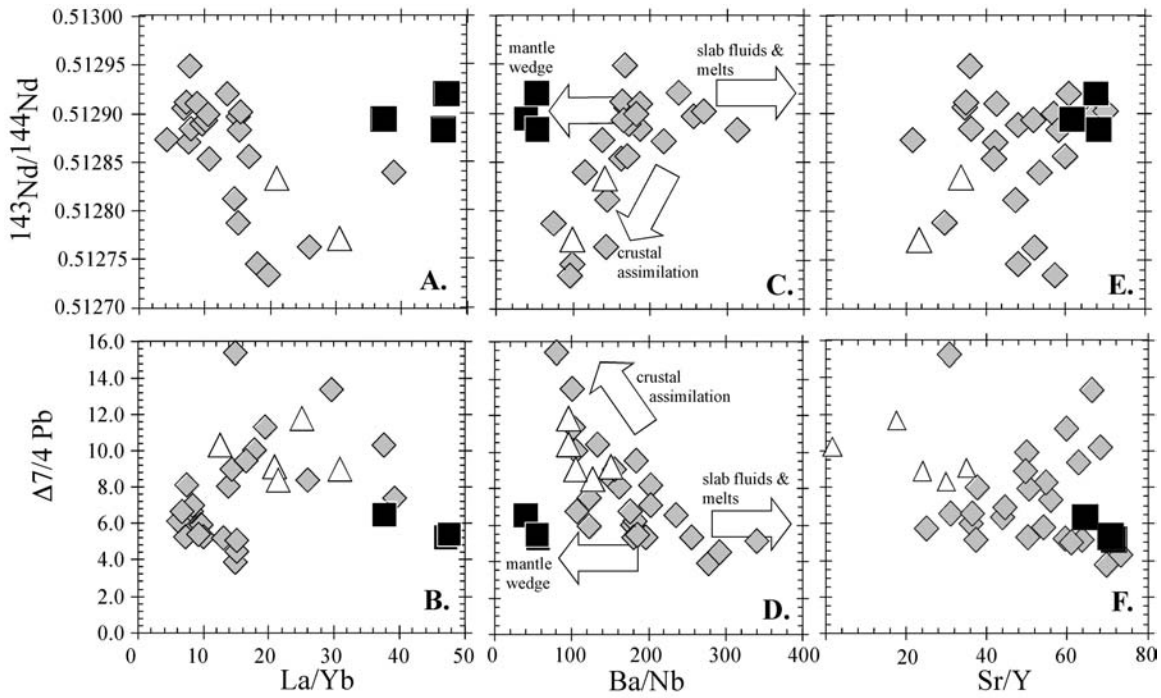
0.51300
0.51295
0.51290
0.51285
0.51280
0.51275
0.51270
143Nd/144Nd
A.
mantle wedge
slab fluids & melts
crustal assimilation
C.
E.
16.0
14.0
12.0
10.0
8.0
6.0
4.0
2.0
0.0
Δ7/4 Pb
B.
crustal assimilation
slab fluids & melts
mantle wedge
D.
F.
0
10
20
30
40
50
La/Yb
0
100
200
300
400
Ba/Nb
20
40
60
80
Sr/Y

FIGURE 15

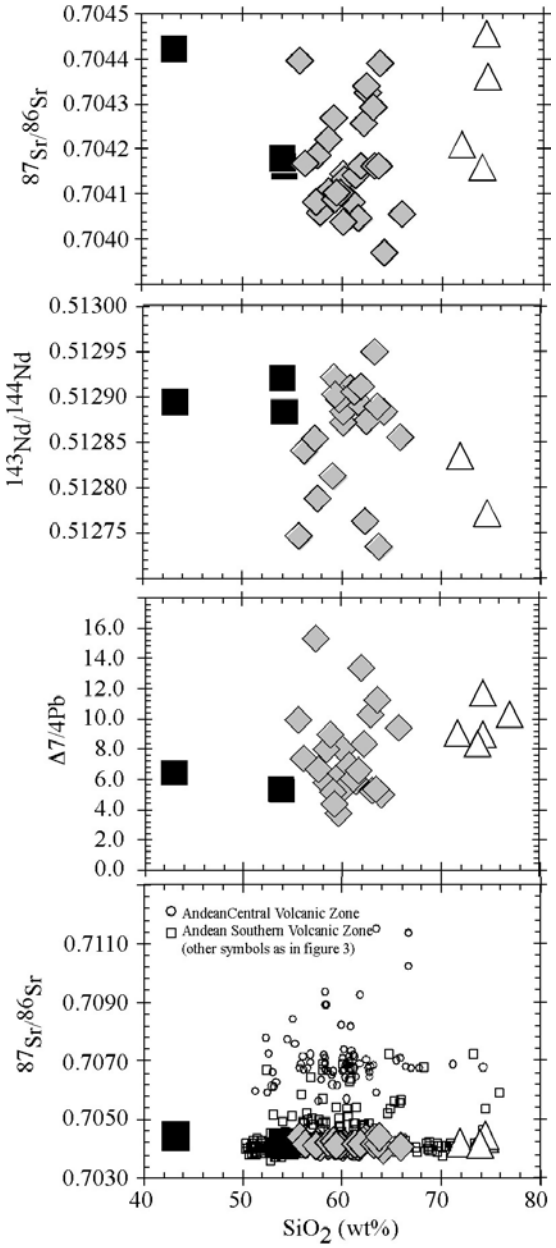
0.7045
0.7044
0.7043
0.7042
0.7041
0.7040
87Sr/86Sr
0.51300
0.51295
0.51290
0.51285
0.51280
0.51275
143Nd/144Nd
16.0
14.0
12.0
10.0
8.0
6.0
4.0
2.0
0.0
Δ7/4Pb
AndeanCentral Volcanic Zone
Andean Southern Volcanic Zone
(other symbols as in figure 3)
0.7110
0.7090
0.7070
0.7050
0.7030
87Sr/86Sr
40
50
60
70
80
SiO2 (wt%)

FIGURE 16

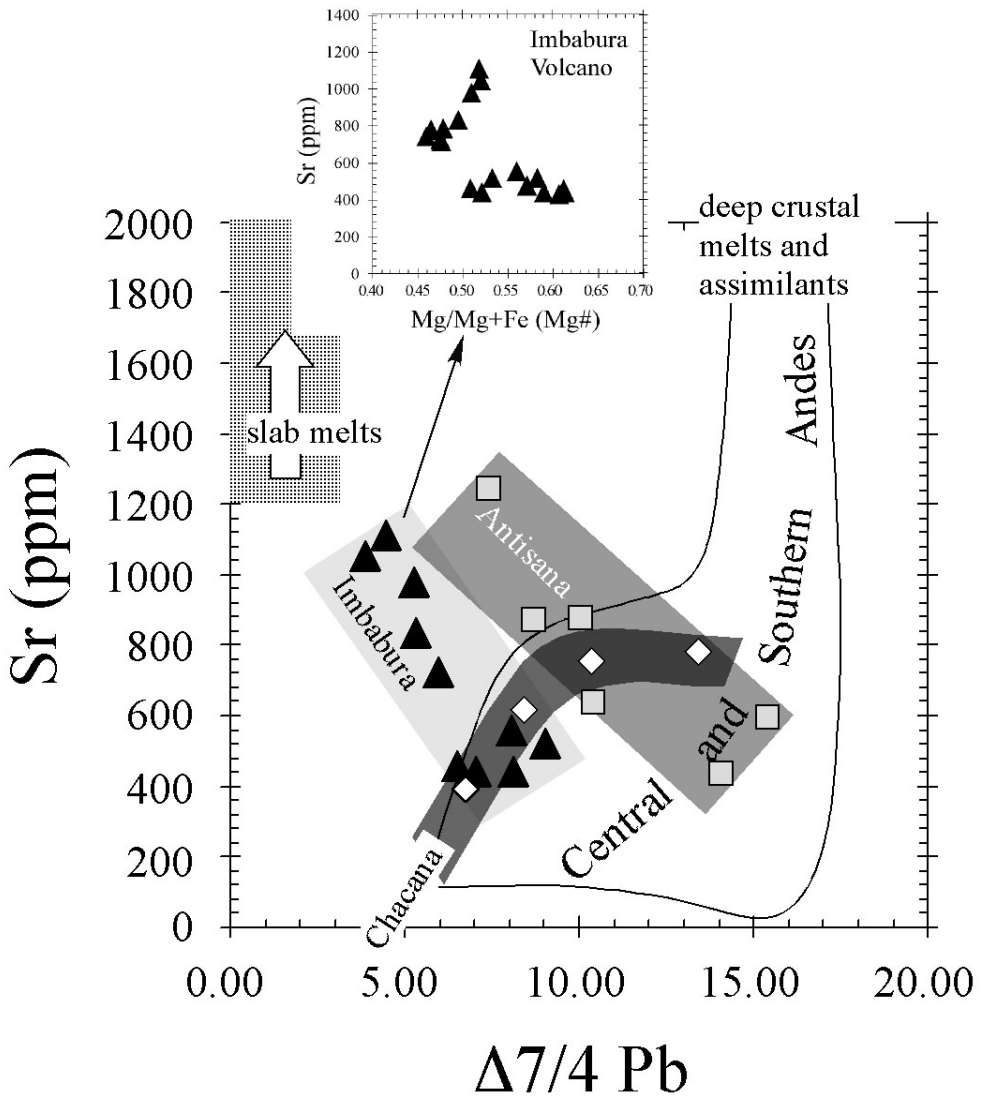
Imbabura
Volcano
Sr (ppm)
Mg/Mg+Fe (Mg#)
deep crustal
melts and
assimilants
slab melts
Antisana
Imbabura
Southern
Andes
and
Central
Chacana
Sr (ppm)
Δ7/4 Pb

FIGURE 17

Table 1- Whole-rock major and trace elements

Rock type	*Basalts and Basaltic-andesites*			*Andesites and Dacites*													
Location	***Sumaco***			***Imbabura***													
Sample	***GS4****	***3D3****	***GS5****	***IMB-1***	***IMB-2***	***IMB-3***	***IMB-4***	***IMB-11***	***IMB-14***	***IMB-16***	***IMB-21.2***	***IMB-22***	***IMB-26***	***IMB-28***	***IMB-29***	***IMB-30***	***IMB-32***	***IMB-36***
SiO_2	54.02	43.24	54.22	59.84	57.76	59.42	60.10	59.30	61.74	61.87	63.46	56.86	60.18	60.90	60.26	58.67	58.10	60.09
TiO_2	0.78	1.72	0.77	0.58	0.63	0.59	0.54	0.59	0.48	0.48	0.52	0.67	0.51	0.51	0.52	0.70	0.58	0.53
Al_2O_3	19.39	15.82	19.67	17.80	17.00	17.74	17.84	17.51	17.73	17.66	16.65	17.91	16.36	16.55	16.20	17.08	16.76	17.60
FeO*	6.30	11.62	6.51	5.84	6.85	6.07	6.18	6.32	5.46	5.46	5.00	7.18	5.83	5.60	5.93	6.26	6.49	6.15
MnO	0.22	0.23	0.22	0.11	0.12	0.12	0.13	0.12	0.12	0.12	0.09	0.12	0.11	0.10	0.11	0.11	0.11	0.13
MgO	1.77	6.31	1.77	3.54	5.11	3.66	3.17	3.68	2.66	2.60	2.90	4.58	5.13	4.59	5.27	4.79	5.59	3.38
CaO	6.31	14.20	6.09	7.00	7.80	7.14	7.25	7.27	6.65	6.63	5.77	7.69	6.78	6.72	6.80	7.06	7.54	7.17
Na_2O	6.62	4.43	6.33	3.67	3.59	3.71	3.63	3.71	3.92	3.95	4.00	3.86	3.71	3.69	3.63	3.69	3.65	3.66
K_2O	4.12	1.05	3.96	1.41	0.99	1.33	0.94	1.26	1.04	1.03	1.48	0.99	1.28	1.21	1.15	1.46	1.03	1.09
P_2O_5	0.47	1.38	0.46	0.21	0.15	0.23	0.22	0.23	0.20	0.21	0.13	0.15	0.12	0.12	0.13	0.19	0.13	0.22
Total	100.0	100.0	100.0	100.0	100.0	100.0	100.0	100.0	100.0	100.0	100.0	100.0	100.0	100.0	100.0	100.0	100.0	100.0
Mg#	0.28	0.43	0.27	0.46	0.51	0.45	0.42	0.45	0.40	0.40	0.45	0.47	0.55	0.53	0.55	0.51	0.54	0.43
Rb	106.1	97.7	107.8	21.3	16.1	21.1	14.9	17.9	17.1	16.2	28.2	17.8	23.3	21.3	24.2	27.3	19.9	15.6
Sr	2597	2582	2560	1051	475	1109	785	978	783	745	462	518	456	442	438	555	430	832
Y	38.4	41.9	37.5	15.7	12.9	15.8	16.2	16.0	15.2	14.5	10.3	13.3	10.8	10.4	12.1	11.4	11.0	14.6
Zr	359	231	353	86	73	87	77	79	85	82	75	76	67	69	76	89	68	69
Nb	54.3	37.9	53.4	3.2	2.7	3.2	3.1	3.0	3.1	3.0	2.6	2.4	2.3	2.7	2.8	3.9	2.1	2.7
Cs	2.79	1.70	2.84	1.19	0.53	1.17	0.60	0.92	0.66	0.63	1.03	0.62	0.72	0.73	0.84	0.81	0.41	0.76
Ba	2797	1435	2800	813	433	858	448	705	515	498	614	467	504	501	515	586	426	495
Hf	6.87	5.39	6.82	2.55	2.06	2.51	2.27	2.36	2.43	2.29	2.20	2.17	1.91	1.98	2.14	2.47	1.95	2.05
Ta	2.98	1.94	2.95	0.19	0.18	0.20	0.20	0.19	0.18	0.18	0.20	0.15	0.17	0.17	0.20	0.25	0.14	0.16
Pb	29.4	12.5	29.9	12.6	4.3	12.5	6.4	10.0	6.3	6.2	4.9	4.5	5.4	4.5	5.6	6.0	4.3	7.2
Th	29.9	18.3	29.4	8.6	1.4	8.9	3.2	7.1	3.5	3.4	1.4	1.3	2.0	2.0	2.0	2.6	1.6	3.7
U	8.7	4.2	9.3	2.6	0.5	2.7	1.1	2.2	1.1	1.1	0.7	0.6	0.7	0.6	0.8	0.7	0.6	1.3
Sc	5	26	5	19	21	17	24	18	8	6	4	24	23	19	23	19	25	18
V	122	343	128	116	165	131	124	143	112	106	110	171	141	137	144	146	158	132
Cr				27	101	36	17	29	22	16	63	33	228	191	260	193	163	20
Ni	24	20	9	17	47	19	9	15	9	10	18	23	75	56	65	52	55	11
Cu				43	44	33	33	31	22	25	17	32	30	31	26	44	40	36
Zn				77	76	74	77	76	72	72	72	77	69	71	67	73	72	74
La	141.40	101.70	139.48	22.90	8.52	23.16	13.55	20.42	14.23	13.62	7.62	7.81	7.77	8.18	8.89	13.13	7.29	14.06
Ce	230.08	186.72	226.50	39.16	16.47	40.09	25.44	35.75	26.32	25.15	14.49	15.36	14.78	15.50	16.90	25.11	14.16	25.86
Pr	23.89	22.00	23.46	4.59	2.09	4.67	3.17	4.24	3.22	3.06	1.88	2.04	1.83	1.91	2.06	3.08	1.80	3.18
Nd	85.59	88.50	84.20	18.87	9.33	19.46	13.77	17.68	13.56	13.08	8.34	9.32	8.03	8.25	8.98	13.06	8.03	13.39
Sm	14.82	17.61	14.48	3.95	2.50	4.04	3.12	3.79	3.05	2.95	2.25	2.52	2.05	2.13	2.22	3.16	2.12	3.07
Eu	4.15	4.99	4.12	1.15	0.81	1.21	0.99	1.13	0.97	0.90	0.73	0.85	0.68	0.70	0.73	0.97	0.70	0.96
Gd	10.39	13.46	10.03	3.17	2.49	3.23	2.92	3.21	2.63	2.57	2.13	2.47	1.95	2.01	2.16	2.78	2.15	2.66
Tb	1.35	1.71	1.32	0.46	0.39	0.48	0.48	0.47	0.42	0.41	0.32	0.40	0.32	0.32	0.35	0.40	0.34	0.41
Dy	7.16	8.74	7.00	2.82	2.35	2.87	2.89	2.84	2.68	2.55	1.90	2.49	1.98	1.99	2.10	2.32	2.05	2.54
Ho	1.31	1.48	1.28	0.59	0.48	0.59	0.59	0.58	0.53	0.53	0.37	0.51	0.40	0.40	0.43	0.44	0.42	0.53
Er	3.33	3.59	3.26	1.55	1.26	1.61	1.59	1.63	1.51	1.44	1.00	1.36	1.11	1.05	1.20	1.10	1.12	1.45
Tm	0.49	0.48	0.48	0.23	0.18	0.23	0.23	0.24	0.23	0.21	0.14	0.19	0.16	0.15	0.18	0.15	0.16	0.21
Yb	3.02	2.73	3.01	1.51	1.15	1.50	1.47	1.52	1.43	1.38	0.89	1.22	1.03	0.93	1.11	0.93	0.99	1.34
Lu	0.47	0.40	0.46	0.24	0.18	0.24	0.24	0.24	0.23	0.22	0.15	0.19	0.15	0.15	0.17	0.15	0.16	0.22
Sr/Y	67.6	61.6	68.4	66.8	36.9	70.1	48.4	61.0	51.5	51.4	45.1	38.8	42.3	42.7	36.3	48.6	39.1	57.0
Ba/Nb	51.5	37.9	52.5	256.5	162.8	269.8	144.1	236.6	168.3	168.8	240.8	192.2	217.2	186.9	187.3	150.6	199.1	182.0
La/Yb	46.8	37.3	46.3	15.2	7.4	15.4	9.2	13.4	10.0	9.9	8.6	6.4	7.5	8.8	8.0	14.1	7.4	10.5

***Major elements and Ni are from Barragan et al (1998)**

Rock type	Andesites and Dacites																	
Location	Imbabura				Puluagua												Quilotoa	Ilalo
Sample	IMB-38	IMB-39	IMB-42	IMB-45	PUL-1	PUL-2	PUL-3	PUL-4	PUL-5	PUL-6	PUL-7	PUL-8	PUL-9	PUL-10	PUL-11	PUL-12	QI-12	II-2
SiO_2	59.13	60.00	62.47	61.70	63.49	63.37	63.06	63.28	62.69	63.68	63.67	63.37	61.34	61.93	61.91	62.29	65.98	57.33
TiO_2	0.68	0.54	0.44	0.48	0.57	0.57	0.57	0.56	0.54	0.51	0.54	0.55	0.62	0.63	0.61	0.61	0.46	0.79
Al_2O_3	17.06	17.93	17.02	17.85	16.56	16.54	16.75	16.67	16.29	16.29	16.96	16.69	15.91	16.16	16.30	16.32	16.99	17.24
FeO*	5.95	6.18	5.27	5.32	5.55	5.63	5.50	5.53	5.36	5.18	5.05	5.39	6.34	6.27	6.13	5.48	3.51	7.05
MnO	0.11	0.13	0.11	0.12	0.09	0.09	0.09	0.09	0.10	0.09	0.08	0.08	0.10	0.10	0.10	0.09	0.07	0.13
MgO	4.66	3.14	3.21	2.71	2.75	2.68	2.85	2.75	3.58	3.12	2.58	2.77	4.38	3.85	3.74	3.88	2.00	5.41
CaO	6.85	7.24	6.25	6.71	5.40	5.41	5.58	5.49	5.77	5.34	5.36	5.37	6.02	5.70	5.78	5.87	4.53	7.16
Na_2O	3.95	3.73	3.83	3.87	4.40	4.51	4.42	4.44	4.37	4.41	4.57	4.57	4.06	4.20	4.22	4.24	4.68	3.71
K_2O	1.42	0.91	1.26	1.04	1.05	1.07	1.05	1.06	1.17	1.24	1.04	1.06	1.07	1.04	1.05	1.07	1.62	1.02
P_2O_5	0.18	0.20	0.13	0.20	0.14	0.14	0.14	0.14	0.13	0.13	0.15	0.15	0.15	0.12	0.15	0.15	0.16	0.16
Total	100.0	100.0	100.0	100.0	100.0	100.0	100.0	100.0	100.0	100.0	100.0	100.0	100.0	100.0	100.0	100.0	100.0	100.0
Mg#	0.52	0.41	0.46	0.41	0.41	0.40	0.42	0.41	0.48	0.45	0.41	0.42	0.49	0.46	0.46	0.49	0.44	0.51
Rb	28.2	13.5	25.5	15.8	15.9	17.1	16.5	16.2	20.4	22.0	16.3	16.1	16.4	15.9	15.7	15.9	30.9	16.3
Sr	518	727	440	720	386	425	416	419	399	397	466	451	423	429	424	436	533	515
Y	10.9	14.6	11.3	13.9	11.6	12.3	12.0	11.7	13.2	12.7	9.7	10.4	12.2	11.6	12.1	11.6	8.9	12.3
Zr	86	72	76	77	76	83	79	79	90	97	79	78	79	81	80	79	88	79
Nb	3.8	2.9	2.8	2.8	2.9	3.1	2.9	3.0	3.0	3.2	2.7	2.7	2.6	2.7	2.8	2.7	3.5	2.9
Cs	0.74	0.51	0.90	0.58	0.35	0.45	0.56	0.48	0.34	0.47	0.42	0.57	0.60	0.62	0.59	0.58	1.65	0.29
Ba	545	416	556	466	467	517	485	494	540	576	465	463	444	454	449	448	589	471
Hf	2.41	2.10	2.18	2.20	2.27	2.52	2.38	2.41	2.58	2.76	2.38	2.35	2.28	2.37	2.30	2.34	2.59	2.27
Ta	0.24	0.18	0.20	0.17	0.20	0.22	0.20	0.21	0.22	0.24	0.19	0.19	0.18	0.18	0.18	0.17	0.29	0.19
Pb	5.9	5.6	5.8	5.9	4.0	4.3	3.9	4.1	4.8	4.8	4.2	4.2	4.1	4.5	4.5	4.1	8.0	4.7
Th	2.7	2.8	2.0	3.1	1.0	1.0	1.0	1.0	1.4	1.6	1.0	1.0	1.0	1.1	1.1	1.1	3.6	2.0
U	0.8	1.0	0.8	1.0	0.5	0.5	0.5	0.5	0.6	0.7	0.5	0.5	0.5	0.5	0.5	0.5	1.4	0.5
Sc	17	15	15	14	16	12	16	11	13	9	10	10	24	17	20	25	8	21
V	158	122	107	114	121	129	126	125	120	114	111	120	145	143	140	144	85	181
Cr	147	21	73	17	26	31	33	32	121	96	35	35	147	103	87	100	14	198
Ni	45	13	22	7	16	11	16	16	35	28	15	16	37	32	29	31	15	76
Cu	39	44	17	25	28	27	26	23	25	28	22	30	9	20	31	23	23	43
Zn	70	75	66	73	75	75	77	74	68	69	72	75	78	77	80	80	63	80
La	12.71	12.99	9.32	13.20	7.75	8.01	7.41	7.77	8.58	9.17	7.83	7.68	7.37	7.47	7.40	7.58	12.11	10.76
Ce	23.96	23.96	17.41	24.52	15.28	16.40	15.45	15.63	16.21	17.07	15.47	15.47	14.97	15.01	15.20	15.45	22.85	22.54
Pr	2.87	3.11	2.11	3.00	2.17	2.22	2.09	2.07	2.11	2.21	2.04	2.05	2.01	2.00	2.04	1.99	2.77	2.68
Nd	12.16	13.00	8.83	12.79	9.88	10.03	9.49	9.40	9.39	9.60	9.28	9.45	9.24	9.10	9.44	9.20	11.42	11.90
Sm	2.88	2.92	2.11	2.81	2.58	2.68	2.55	2.57	2.46	2.46	2.40	2.47	2.51	2.42	2.52	2.45	2.58	3.06
Eu	0.86	0.94	0.69	0.91	0.78	0.83	0.82	0.81	0.74	0.74	0.77	0.75	0.79	0.78	0.81	0.76	0.74	1.00
Gd	2.53	2.67	2.04	2.55	2.51	2.64	2.52	2.51	2.40	2.38	2.24	2.37	2.50	2.46	2.55	2.42	2.18	2.89
Tb	0.37	0.42	0.33	0.39	0.39	0.40	0.39	0.38	0.39	0.39	0.34	0.35	0.39	0.37	0.39	0.37	0.30	0.43
Dy	2.16	2.59	1.99	2.41	2.22	2.36	2.25	2.26	2.38	2.27	1.89	1.97	2.36	2.21	2.23	2.18	1.69	2.50
Ho	0.40	0.52	0.40	0.49	0.43	0.46	0.44	0.43	0.47	0.46	0.36	0.39	0.45	0.44	0.45	0.41	0.33	0.49
Er	1.04	1.45	1.14	1.37	1.14	1.21	1.16	1.10	1.29	1.28	0.95	0.99	1.23	1.18	1.18	1.12	0.81	1.21
Tm	0.14	0.21	0.17	0.20	0.16	0.17	0.16	0.16	0.19	0.18	0.13	0.14	0.18	0.17	0.17	0.16	0.12	0.17
Yb	0.87	1.37	1.04	1.30	0.98	0.99	1.00	0.99	1.22	1.18	0.81	0.84	1.09	1.02	1.03	1.01	0.72	1.01
Lu	0.13	0.21	0.17	0.21	0.15	0.16	0.16	0.16	0.20	0.18	0.12	0.14	0.17	0.17	0.17	0.16	0.11	0.16
Sr/Y	47.6	49.8	38.9	51.9	33.2	34.6	34.7	36.0	30.2	31.3	48.1	43.2	34.7	36.9	35.1	37.6	60.1	42.0
Ba/Nb	144.2	141.5	202.2	165.2	162.7	165.7	165.0	167.5	177.6	177.8	172.2	169.6	168.2	166.3	163.3	167.2	169.7	161.3
La/Yb	14.6	9.5	9.0	10.2	7.9	8.1	7.4	7.8	7.0	7.8	9.7	9.1	6.8	7.3	7.2	7.5	16.8	10.7

Rock type	Andesites and Dacites											Rhyolites				
Location	Antisana			Atacazo		Sangay	Pichincha	Chacana				Cotopaxi		Chacana		Chalupas
Sample	3D1 An*	2G3T-A*	HHV	At 02*	957g*	Sg-13	GP-1	Ch-3	Ch-6	Ch-7	Ch-8	Cx-9	Cx-10	Ch-4	Ch-5	Cl-11
SiO_2	56.29	55.76	57.57	58.65	62.57	63.81	64.26	57.78	62.40	62.19	63.11	73.98	71.96	77.23	74.57	74.46
TiO_2	1.04	1.06	0.91	0.66	0.62	0.49	0.39	0.78	0.72	0.80	0.76	0.19	0.25	0.15	0.21	0.24
Al_2O_3	15.59	18.23	16.02	16.21	16.48	17.16	16.90	16.20	17.12	16.42	16.62	14.87	15.62	12.79	14.22	14.13
FeO*	7.29	7.56	6.71	7.75	6.63	3.84	4.47	6.90	4.95	4.97	4.64	1.28	1.81	0.78	1.09	1.24
MnO	0.11	0.12	0.12	0.12	0.09	0.09	0.09	0.12	0.08	0.09	0.08	0.08	0.08	0.05	0.06	0.05
MgO	5.26	3.94	5.86	4.96	2.69	2.60	2.55	6.40	2.69	3.14	2.65	0.45	0.61	0.16	0.28	0.38
CaO	7.17	7.14	6.91	6.80	5.64	4.50	5.24	7.23	5.53	5.57	5.22	1.67	2.31	0.38	1.20	1.26
Na_2O	3.72	4.18	3.58	3.84	4.10	4.26	4.19	3.18	4.15	4.21	4.24	4.56	4.57	4.24	4.38	3.58
K_2O	2.99	1.68	2.10	0.87	1.06	2.98	1.78	1.27	2.14	2.34	2.41	2.83	2.66	4.19	3.95	4.63
P_2O_5	0.54	0.32	0.23	0.14	0.13	0.28	0.13	0.13	0.22	0.27	0.26	0.09	0.12	0.03	0.04	0.04
Total	100.0	100.0	100.0	100.0	100.0	100.0	100.0	100.0	100.0	100.0	100.0	100.0	100.0	100.0	100.0	100.0
Mg#	0.50	0.42	0.55	0.47	0.36	0.48	0.44	0.56	0.43	0.47	0.44	0.33	0.32	0.22	0.26	0.30
Rb	86.0	37.5	73.9	21.9	17.2	96.6	40.0	34.3	61.3	61.5	59.9	71.4	63.6	125.3	125.8	182.0
Sr	1245	875	594	438	355	894	534	399	609	777	749	288	353	33	236	221
Y	23.2	18.2	18.0	18.2	16.4	15.6	9.2	13.3	11.6	12.3	11.5	10.0	10.5	16.3	10.2	12.8
Zr	240	132	145	120	77	140	81	77	127	114	127	119	128	106	145	169
Nb	11.2	8.0	8.3	4.2	2.8	11.0	2.5	4.4	5.8	8.7	8.2	7.4	6.5	12.1	11.2	11.6
Cs	2.95	0.67	3.67	0.73	0.42	4.63	1.02	0.91	1.57	2.54	2.22	2.75	2.67	5.87	5.45	9.77
Ba	1283	782	614	485	387	1054	782	442	822	819	1021	878	912	1082	1096	1047
Hf	6.36	3.70	4.08	3.43	2.26	3.85	2.39	2.32	3.57	3.37	3.56	3.50	3.61	3.81	4.22	5.25
Ta	0.71	0.49	0.95	0.30	0.21	0.95	0.18	0.39	0.40	0.69	0.60	0.68	0.53	1.02	1.10	1.23
Pb	16.8	8.7	11.7	5.2	4.0	19.9	6.8	6.1	11.2	11.8	12.2	12.6	11.9	19.8	19.9	23.2
Th	17.1	4.9	11.9	1.0	0.2	14.3	3.1	4.2	7.9	9.5	10.2	7.4	6.7	12.8	15.6	21.5
U	4.8	1.4	4.4	0.7	0.5	6.1	1.1	1.7	2.0	3.3	2.8	3.3	2.4	4.3	5.7	9.1
Sc	19	18	20	23	26	9	11	24	12	13	11	2	3	3	236	2
V	183	186	165	188	135	85	111	182	132	126	126	7	12	5	12	10
Cr			252			61	33	246	28	49	23	0	0	0	0	0
Ni	71	18	92	47	20	37	23	93	15	27	19	3	4	4	3	2
Cu			55				41	45	17	38	41			3	4	5
Zn			80				61	77	71	77	70			45	37	39
La	60.90	26.51	23.98	11.85	6.83	28.28	11.95	10.32	22.80	27.14	31.94	20.25	20.87	20.44	31.26	32.16
Ce	110.26	49.34	45.21	24.40	13.74	49.64	20.88	19.95	40.88	48.74	55.07	36.34	36.80	38.12	51.49	53.65
Pr	13.13	5.81	5.28	3.26	1.89	5.46	2.43	2.45	4.73	5.51	5.95	3.99	4.02	4.28	5.08	5.60
Nd	52.81	24.25	21.58	15.00	8.73	21.12	9.92	10.44	18.55	21.77	22.89	14.77	14.87	15.01	16.91	19.56
Sm	10.53	5.30	4.79	3.97	2.54	4.11	2.28	2.77	3.94	4.52	4.42	2.80	2.88	3.49	2.90	3.52
Eu	2.73	1.57	1.24	1.14	0.84	0.98	0.68	0.92	1.11	1.22	1.23	0.65	0.72	0.43	0.61	0.64
Gd	7.68	4.45	4.17	3.88	2.83	3.19	1.99	2.72	3.12	3.52	3.30	2.11	2.29	2.74	2.05	2.64
Tb	0.95	0.65	0.62	0.60	0.49	0.46	0.30	0.44	0.44	0.46	0.45	0.31	0.32	0.49	0.31	0.39
Dy	4.76	3.59	3.49	3.49	2.99	2.69	1.78	2.62	2.35	2.52	2.34	1.76	1.84	2.96	1.73	2.27
Ho	0.83	0.66	0.68	0.67	0.62	0.53	0.34	0.52	0.43	0.45	0.41	0.35	0.36	0.57	0.35	0.43
Er	2.02	1.75	1.73	1.75	1.69	1.48	0.90	1.37	1.08	1.13	1.05	0.94	1.01	1.54	0.97	1.21
Tm	0.27	0.24	0.26	0.25	0.26	0.22	0.13	0.20	0.15	0.15	0.15	0.14	0.15	0.25	0.15	0.18
Yb	1.57	1.47	1.58	1.49	1.60	1.44	0.78	1.20	0.88	0.92	0.86	0.94	0.99	1.58	1.02	1.28
Lu	0.24	0.22	0.24	0.24	0.25	0.23	0.12	0.19	0.15	0.15	0.14	0.15	0.17	0.24	0.16	0.20
Sr/Y	53.6	48.0	33.1	24.1	21.6	57.3	58.4	30.0	52.5	63.4	65.4	28.8	33.7	2.0	23.3	17.2
Ba/Nb	114.3	97.9	74.4	114.4	137.7	95.9	314.1	100.0	142.5	93.9	124.1	118.8	140.3	89.3	97.9	90.1
La/Yb	38.8	18.0	15.2	8.0	4.3	19.6	15.3	8.6	25.9	29.5	37.1	21.5	21.1	12.9	30.6	25.1

Table 2- Whole-rock Sr, Pb and Nd isotope ratios

Rock type	Location	Sample	$^{87}Sr/^{86}Sr$	$^{206}Pb/^{204}Pb$	$^{207}Pb/^{204}Pb$	$^{208}Pb/^{204}Pb$	$^{143}Nd/^{144}Nd$	εNd	Δ7/4
Basalt	Sumaco	**GS5**	0.704162	18.792	15.581	38.520	0.512884	4.79	5.27
Basaltic-andesite	Sumaco	**3D3**	0.704422	18.872	15.602	38.660	0.512895	5.02	6.50
Basaltic-andesite	Sumaco	**GS4**	0.704179	18.796	15.583	38.529	0.512921	5.51	5.47
Andesite	Imbabura	**IMB-1**	0.704104	19.098	15.600	38.770	0.512897	5.05	3.88
Andesite	Imbabura	**IMB-3**	0.704103	19.099	15.606	38.786	0.512902	5.15	4.47
Andesite	Imbabura	**IMB-11**	0.704088	19.072	15.611	38.766	0.512921	5.53	5.26
Andesite	Imbabura	**IMB-26**	0.704143	18.921	15.607	38.614	0.512871	4.55	6.49
Andesite	Imbabura	**IMB-28**	0.704083	18.953	15.616	38.657	0.512910	5.31	7.05
Andesite	Imbabura	**IMB-29**	0.704132	18.974	15.629	38.717	0.512884	4.81	8.12
Andesite	Imbabura	**IMB-30**	0.704222	18.913	15.622	38.677			8.08
Andesite	Imbabura	**IMB-36**	0.704038	19.123	15.617	38.833	0.512900	5.11	5.31
Andesite	Imbabura	**IMB-38**	0.704269	18.900	15.630	38.712	0.512812	3.40	9.03
Andesite	Imbabura	**IMB-45**	0.704045	19.073	15.618	38.784	0.512893	4.97	5.95
Dacite	Puluagua	**PUL-4**	0.704162	18.921	15.595	38.572	0.512949	6.06	5.29
Dacite	Puluagua	**PUL-7**	0.704162	18.921	15.596	38.572	0.512889	4.90	5.39
Andesite	Puluagua	**PUL-9**	0.704140	18.934	15.605	38.610	0.512906	5.23	6.15
Andesite	Puluagua	**PUL-11**	0.704162	18.893	15.606	38.562	0.512912	5.34	6.70
Dacite	Quilotoa	**QI-12**	0.704056	18.985	15.644	38.750	0.512856	4.26	9.50
Andesite	Ilalo	**Il-2**	0.704082				0.512854	4.21	
Andesite	Antisana	**3D1An**	0.704167	18.936	15.618	38.728	0.512840	3.93	7.48
Andesite	Antisana	**2G3T-A**	0.704397	18.924	15.643	38.762	0.512746	2.11	10.05
Andesite	Antisana	**HHV**	0.704186	18.985	15.703	38.978	0.512788	2.92	15.42
Andesite	Atacazo	**At 02**	0.704107	18.933	15.602	38.619			5.83
Andesite	Atacazo	**957g**	0.704324				0.512873	4.58	
Dacite	Sangay	**Sg-13**	0.704391	18.816	15.644	38.754	0.512734	1.86	11.39
Dacite	Pichincha	**GP-1**	0.703970	18.958	15.597	38.698	0.512883	4.79	5.04
Andesite	Chacana	**CH-3**	0.704059	18.956	15.613	38.680			6.75
Andesite	Chacana	**CH-6**	0.704339	18.983	15.633	38.755	0.512763	2.43	8.41
Andesite	Chacana	**CH-7**	0.704257	19.028	15.688	38.947			13.45
Dacite	Chacana	**CH-8**	0.704292	18.925	15.646	38.694			10.32
Rhyolite	Cotopaxi	**CX-9**	0.704158	18.963	15.631	38.710			8.41
Rhyolite	Cotopaxi	**CX-10**	0.704210	18.951	15.637	38.716	0.512834	3.83	9.22
Rhyolite	Chacana	**CH-4**		18.925	15.646	38.775			10.33
Rhyolite	Chacana	**CH-5**	0.704360	18.918	15.632	38.732	0.512771	2.59	9.04
Rhyolite	Chalupas	**Cl-11**	0.704455	18.993	15.668	38.873			11.77

7/4NHRL
15.52807
15.53673
15.52846
15.56119
15.5613
15.55837
15.54207
15.54555
15.54783
15.5412
15.56391
15.53979
15.55848
15.54203
15.54207
15.54348
15.53903
15.54898

15.54369
15.54239
15.54897
15.54338

15.5306
15.54609
15.54582
15.54875
15.55359
15.54251
15.54662
15.54529
15.5425
15.5417
15.54987

#REF!
#REF!
#REF!
#REF!
#REF!
#REF!

87/86Sr	6/4Pb	7/4Pb	8/4Pb	143/144Nd	Eps Nd
±	±	±	±	±	±
9.86E-06	0.023	0.028	0.093	2.26E-05	0.44
9.86E-06	0.023	0.028	0.093	2.36E-05	0.46
9.86E-06	0.023	0.028	0.093	9.23E-06	0.18
1.13E-05	0.023	0.028	0.093	6.15E-06	0.12
9.86E-06	0.023	0.028	0.093	6.15E-06	0.12
8.45E-06	0.023	0.028	0.093	7.18E-06	0.14
8.45E-06	0.023	0.028	0.093	8.21E-06	0.16
1.13E-05	0.023	0.028	0.093	8.21E-06	0.16
9.86E-06	0.023	0.028	0.093	1.13E-05	0.22
9.86E-06	0.023	0.028	0.093	8.21E-06	0.16
1.13E-05	0.023	0.028	0.093		
1.13E-05	0.023	0.028	0.093	7.18E-06	0.14
8.45E-06	0.023	0.028	0.093	8.20E-06	0.16
9.86E-06	0.023	0.028	0.093	9.23E-06	0.18
9.86E-06	0.023	0.028	0.093	8.20E-06	0.16
1.13E-05	0.023	0.028	0.093	1.13E-05	0.22
1.27E-05	0.023	0.028	0.093	7.18E-06	0.14
1.13E-05				1.33E-05	0.26
1.13E-05	0.023	0.028	0.093		
1.13E-05	0.023	0.028	0.093		
	0.023	0.028	0.093		
1.13E-05	0.023	0.028	0.093	1.13E-05	0.22
1.27E-05	0.023	0.028	0.093	8.20E-06	0.16
9.86E-06	0.023	0.028	0.093		
1.13E-05	0.023	0.028	0.093		
1.27E-05	0.023	0.028	0.093		
9.86E-06	0.023	0.028	0.093		
9.86E-06	0.023	0.028	0.093	9.23E-06	0.18
1.13E-05	0.023	0.028	0.093	1.95E-05	0.38
9.86E-06	0.023	0.028	0.093	1.03E-05	0.2
9.86E-06	0.023	0.028	0.093	1.44E-05	0.28
1.13E-05	0.023	0.028	0.093	7.18E-06	0.14
9.86E-06				8.21E-06	0.16
1.13E-05	0.023	0.028	0.093	8.21E-06	0.16
1.13E-05	0.023	0.028	0.093	2.05E-05	0.4